U.S. DEPARTMENT OF ENERGY | Office of Science

DOE/SC-ARM-16-006

Aerosol and Cloud Experiments in Eastern North Atlantic (ACE-ENA) Science Plan

J Wang
X Dong
R Wood

April 2016

ARM
CLIMATE RESEARCH FACILITY

DISCLAIMER

This report was prepared as an account of work sponsored by the U.S. Government. Neither the United States nor any agency thereof, nor any of their employees, makes any warranty, express or implied, or assumes any legal liability or responsibility for the accuracy, completeness, or usefulness of any information, apparatus, product, or process disclosed, or represents that its use would not infringe privately owned rights. Reference herein to any specific commercial product, process, or service by trade name, trademark, manufacturer, or otherwise, does not necessarily constitute or imply its endorsement, recommendation, or favoring by the U.S. Government or any agency thereof. The views and opinions of authors expressed herein do not necessarily state or reflect those of the U.S. Government or any agency thereof.

DOE/SC-ARM-16-006

Aerosol and Cloud Experiments in Eastern North Atlantic (ACE-ENA) Science Plan

J Wang, Brookhaven National Laboratory
Principal Investigator

Xiquan Dong, University of North Dakota
Robert Wood, University of Washington
Co-Principal Investigators

April 2016

Work supported by the U.S. Department of Energy,
Office of Science, Office of Biological and Environmental Research

Abstract

With their extensive coverage, low clouds greatly impact global climate. Presently, low clouds are poorly represented in global climate models (GCMs), and the response of low clouds to changes in atmospheric greenhouse gases and aerosols remains the major source of uncertainty in climate simulations. The poor representations of low clouds in GCMs are in part due to inadequate observations of their microphysical and macrophysical structures, radiative effects, and the associated aerosol distribution and budget in regions where the aerosol impact is the greatest. The Eastern North Atlantic (ENA) is a region of persistent but diverse subtropical marine boundary-layer (MBL) clouds, whose albedo and precipitation are highly susceptible to perturbations in aerosol properties. Boundary-layer aerosol in the ENA region is influenced by a variety of sources, leading to strong variations in cloud condensation nuclei (CCN) concentration and aerosol optical properties.

Recently a permanent ENA site was established by the U.S. Department of Energy (DOE)'s Atmospheric Radiation Measurement (ARM) Climate Research Facility on Graciosa Island in the Azores, providing invaluable information on MBL aerosol and low clouds. At the same time, the vertical structures and horizontal variabilities of aerosol, trace gases, cloud, drizzle, and atmospheric thermodynamics are critically needed for understanding and quantifying the budget of MBL aerosol, the radiative properties, precipitation efficiency, and lifecycle of MBL clouds, and the cloud response to aerosol perturbations. Much of this data can be obtained only through aircraft-based measurements. In addition, the interconnected aerosol and cloud processes are best investigated by a study involving simultaneous in situ aerosol, cloud, and thermodynamics measurements. Furthermore, in situ measurements are also necessary for validating and improving ground-based retrieval algorithms at the ENA site.

This project is motivated by the need for comprehensive in situ characterizations of boundary-layer structure, and associated vertical distributions and horizontal variabilities of low clouds and aerosol over the Azores. ARM Aerial Facility (AAF) Gulfstream-1 (G-1) aircraft will be deployed at the ENA site during two intensive operational periods (IOPs) of early summer (June to July) of 2017 and winter (January to February) of 2018, respectively. Deployments during both seasons allow for examination of key aerosol and cloud processes under a variety of representative meteorological and cloud conditions. The science themes for the deployments include: 1) Budget of MBL CCN and its seasonal variation; 2) Effects of aerosol on cloud and precipitation; 3) Cloud microphysical and macrophysical structures, and entrainment mixing; 4) Advancing retrievals of turbulence, cloud, and drizzle; and 5) Model evaluation and processes studies.

A key advantage of the deployments is the strong synergy between the measurements onboard the G-1 and the routine measurements at the ENA site, including state-of-the-art profiling and scanning radars. The 3D cloud structures provided by the scanning radars will put the detailed in situ measurements into mesoscale and cloud lifecycle contexts. On the other hand, high quality in situ measurements will enable validation and improvements of ground-based retrieval algorithms at the ENA site, leading to high-quality and statistically robust data sets from the routine measurements. The deployments, combined with the routine measurements at the ENA site, will have a long lasting impact on the research and modeling of low clouds and aerosols in the remote marine environment.

Acknowledgments

Principal Investigator (PI)
Jian Wang, Brookhaven National Laboratory

Co-Principal Investigators (Alphabetical)
Xiquan Dong, University of North Dakota
Robert Wood, University of Washington, Seattle

Co-Investigators (Alphabetical)
Eduardo Azevedo, Universidade dos Açores, Portugal
Chris Bretherton, University of Washington, Seattle
Duli Chand, Pacific Northwest National Laboratory
Christine Chiu, University of Reading, United Kingdom
Jerome Fast, Pacific Northwest National Laboratory
Andrew Gettelman, National Center for Atmospheric Research
Steve Ghan, Pacific Northwest National Laboratory
Scott Giangrande, Brookhaven National Laboratory
Mary Gilles, Lawrence Berkeley National Laboratory
Anne Jefferson, CIRES, University of Colorado, Boulder
Mike Jensen, Brookhaven National Laboratory
Pavlos Kollias, McGill University, Canada
Chongai Kuang, Brookhaven National Laboratory
Alex Laskin, Pacific Northwest National Laboratory
Ernie Lewis, Brookhaven National Laboratory
Xiaohong Liu, University of Wyoming
Yangang Liu, Brookhaven National Laboratory
Ed Luke, Brookhaven National Laboratory
Allison McComiskey, NOAA Earth System Research Laboratory
Fan Mei, Pacific Northwest National Laboratory
Mark Miller, Rutgers University
Arthur Sedlacek, Brookhaven National Laboratory
Raymond Shaw, Michigan Technological University

Collaborators (Alphabetical)
Michael Behrenfeld, Oregon State University
Chris Hostetler, NASA Langley Research Center
Claudio Mazzoleni, Michigan Technological University
Holger Siebert, Leibniz Institute for Tropospheric Research, Germany

Date and location of activities
Deployment of the ARM Aerial Facility Gulfstream-1 aircraft to the ENA site during summer (June-July) of 2017 and winter (January-February) of 2018.

Acronyms and Abbreviations

AAF	ARM Aerial Facility
ACAPEX	ARM Cloud Aerosol Precipitation Experiment
ACME	Accelerated Climate Model for Energy
ACRF	ARM Climate Research Facility
ACTOS	Airborne Cloud Turbulence Observation System
AMF	ARM Mobile Facility
AMS	Aerosol Mass Spectrometer
ARM	Atmospheric Radiation Measurement Climate Research Facility
ASR	Atmospheric System Research
ASTEX	Atlantic Stratocumulus Transition Experiment
CAM	Community Atmosphere Model
CAPI	Cloud-Aerosol-Precipitation Interactions
CAP-MBL	Clouds-Aerosols-Precipitation Marine Boundary Layer
CAPS	Cloud, Aerosol, and Precipitation Spectrometer
CAS	Cloud and Aerosol Spectrometer
CCD	charge-coupled device
CCN	cloud condensation nuclei
CCNPROF	Cloud Condensation Nuclei Profile, an ARM VAP
CESM	Community Earth System Model
CloudSat	A NASA satellite mission to study cloud
COPS	Convective and Orographically Induced Precipitation Study
CPC	Condensation Particle Counter
CVI	Counter-Flow Virtual Impactor
DOE	U.S. Department of Energy
ECMWF	European Centre for Medium-Range Weather Forecasts
EIL	Entrainment Interfacial Layer
EMSL	Environmental Molecular Science Laboratory
ENA	Eastern North Atlantic
ENCORE	ENsemble ClOud Retrieval
EPIC	East Pacific Investigation of Climate
EVS	Earth Venture Suborbital
FCDP	Fast Cloud Droplet Probe
FFT	fast Fourier transform
FIMS	Fast Integrated Mobility Spectrometer
FT	free troposphere
GCM	global climate model

GCSS	GEWEX Cloud Systems Study
GERB	Geostationary Earth Radiation Budget
GEWEX	Global Energy and Water Cycle Experiment
GFS	Global Forecast System
GLOMAP	an aerosol microphysics model
GPCI	GCSS Pacific Cross-Section Intercomparison
HOLODEC	Holographic Detector for Clouds
HR-ToF-AMS	High-Resolution Time-of-Flight Aerosol Mass Spectrometer
HVPS-3	High-Volume Precipitation Spectrometer Version 3
IOP	intensive operational period
LES	large-eddy simulations
LWC	liquid water content
LWP	liquid water path
MACC	Monitoring Atmospheric Composition and Climate
MAGIC	Marine ARM GPCI Investigation of Clouds
MBL	marine boundary layer
MODIS	Moderate Resolution Imaging Spectroradiometer
NAAMES	North Atlantic Aerosols and Marine Ecosystems Study
NASA	National Aeronautics and Space Administration
NPF	new particle formation
PCASP	Passive Cavity Aerosol Spectrometer
PI	Principal Investigator
PILS	Particle-Into-Liquid Sampler
PMO	Pico Mountain Observatory
PNNL	Pacific Northwest National Laboratory
PSAP	Particle Soot Absorption Photometer
PTR-MS	Proton Transfer Reaction-Mass Spectrometer
RHI	Range Height Indicator
RICO	Rain in Cumulus over the Ocean
SACR	Scanning ARM Cloud Radar
SMPS	Scanning Mobility Particle Sizer
SP2	Single-Particle Soot Photometer
SSA	sea spray aerosol
TCAP	Two-Column Aerosol Project
UCPC	Ultrafine Condensation Particle Counter
UHF	ultra-high frequency
UHSAS	Ultra-High-Sensitivity Aerosol Spectrometer
VAMOS	Variability of the American Monsoon System

VAP	Value-Added Product
VOC	volatile organic compound
VOCALS-REx	VAMOS Ocean-Cloud-Atmosphere-Land Study-Regional Experiment
WRF	Weather Research and Forecasting
WRF-Chem	Weather Research and Forecasting-Chemistry Version
XSAPR2	X-Band Scanning ARM Precipitation Radar
2D-S	Two-Dimensional Stereo Probe

Contents

Abstract ... iii
Acknowledgments ... iv
Acronyms and Abbreviations ... v
1.0 Project Descriptions ... 1
1.1 Motivation and Background ... 1
1.1.1 New Ground-Based, Long-Term Measurements at the ENA Site ... 2
1.1.2 Budget of MBL CCN and its Seasonal Variation ... 2
1.1.3 Effects of Aerosol on Clouds and Precipitation ... 5
1.1.4 Cloud Microphysical and Macrophysical Structures, and Entrainment Mixing ... 8
1.1.5 Advancing Retrievals of Turbulence, Clouds, and Drizzle ... 10
1.2 Scientific Objectives ... 11
1.3 Deployment Strategies ... 12
1.3.1 Instruments and Measurements Onboard G-1 ... 13
1.3.2 Flight Plans ... 14
1.3.3 Surface Measurements ... 16
1.4 Synergistic Activities and Coordination with Other Studies ... 16
2.0 Scientific Objectives and Research ... 17
2.1 Budget of MBL CCN and its Seasonal Variation ... 17
2.1.1 Contributions from Different Sources and their Seasonal Variations ... 17
2.1.2 Removal of MBL CCN by Droplet Coalescence Scavenging ... 19
2.2 Effects of Aerosol on Clouds and Precipitation ... 19
2.2.1 The Representativeness of Surface Measurements for CCN at Cloud Base ... 19
2.2.2 Impact of Aerosol on Cloud Microphysics and Precipitation ... 20
2.3 Cloud Microphysical and Macrophysical Structures, and Entrainment Mixing ... 21
2.3.1 Cloud Microphysical and Macrophysical Structures ... 21
2.3.2 Entrainment Mixing ... 22
2.4 Advancing Retrievals of Turbulence, Cloud, and Drizzle ... 23
2.4.1 Validating Retrievals from Vertically Pointing Observations ... 23
2.4.2 3D Cloud and Drizzle Retrievals from Scanning Radars ... 25
2.5 Model Evaluation and Processes Studies ... 25
2.5.1 Comparison of Model Simulations with Observations ... 25
2.5.2 Understanding the Controlling Processes for Aerosol Budget, Cloud Lifecycle, and Aerosol Cloud Interactions Using Validated/Constrained Model Simulations ... 27
3.0 Relevancy ... 27
4.0 References ... 28
5.0 ARM Resources Required ... 35
5.1 ARM Aerial Facilities ... 36

5.2 ARM Ground Facilities 37
5.3 EMSL/ALS Resources 38

Figures

1. (a) Annual mean aerosol first indirect forcing, and (b) uncertainty in simulated first indirect forcing due to uncertainty in model (GLOMAP) parameters. 1
2. Map showing the location of the Azores in the Eastern North Atlantic. 2
3. Major sources of boundary-layer CCN in a remote marine environment such as the ENA. 3
4. Composite seasonal cycles of (a) Surface CCN concentrations at four supersaturations. (b) Aerosol total and submicron dry extinction. (c) Monthly-mean aerosol optical depth and percentile values from the Cimel sun photometer and mean values from MODIS. 4
5. Diagram of open mesoscale cellular convection structure with an ultra-clean aerosol layer towards the top of the boundary layer. 5
6. Cloud droplet concentration from the MODIS satellite plotted as a function of CCN concentration measured on Graciosa during the CAP-MBL deployment (2009-2010). 6
7. Cloud droplet concentration plotted as a function of cloud base aerosol concentration for measurements during summer 1992 during ASTEX in the vicinity of the Azores. 7
8. Horizontal cross section of 5-cm radar reflectivity at 1-km elevation during a heavy drizzle period and time–height plot of 8-mm radar reflectivity above the ship during EPIC 2001. 9
9. Retrieved cloud fields for (left) stratocumulus case and (right) cumulus case. 11
10. Flight plan for characterizing the vertical structure and mesoscale variation of thermodynamics, aerosol, cloud, and precipitation. 14
11. Electron microscopy and X-ray spectromicroscopy images illustrating morphology and the internal composition of particles from various sources collected in field studies. 18
12. Precipitation intensity susceptibility with respect to CCN number concentration as a function of liquid water path in AMF observations during CAP-MBL and COPS and to cloud droplet number concentration in VOCALS observations, and large-eddy simulations of precipitating cumulus initialized using soundings from RICO. 21
13. Retrieved cloud properties in predominantly drizzling conditions on 17 September 2009 at the Azores from the ENCORE method98. 24

Tables

1. Requested instrumentation for the G-1 aircraft. 36
2. Requested instrumentation for ground deployment. 37

1.0 Project Descriptions

1.1 Motivation and Background

The responses of low cloud systems to changes in atmospheric greenhouse gases and aerosols are major sources of uncertainty that limit our ability to predict future climate[1-3]. Climate models disagree substantially in the magnitude of cloud feedback for the regimes of subtropical marine low clouds[1,4], and suffer from the so-called "too few, too bright" problem[5-7]. The "too few" problem, an underestimate in cloud amount, allows more solar radiation to reach the surface. The "too bright" problem, an overestimate in cloud albedo due, for example, to an overestimate in the amount of liquid water within the cloud, causes more sunlight to be reflected. These inaccurate cloud properties lead to an apparently realistic radiation budget due to compensating errors, but overly reflective clouds may result in a significant underestimate in the strength of a negative cloud feedback process involving increased cloud liquid water with warming[8]. Additionally, the interdependence between cloud macrophysical, microphysical, and radiative properties strongly links to the stages of warm cloud and precipitation evolution[9], and could be modified by ambient aerosols[2,10-12]. Remote marine low-cloud systems have large spatial coverage and are particularly susceptible to perturbations in aerosols associated with anthropogenic emissions because of their relatively low optical thickness and background aerosol concentrations (e.g., see Figure 1)[13,14]. Indeed, recent studies find that a large fraction of the global aerosol indirect forcing can be attributed to changes in marine low clouds[15], despite their relatively long distance from most anthropogenic sources. There remain large uncertainties in the magnitude of the global aerosol radiative forcing[2,16,17]. Major contributions to this uncertainty derive from poor understanding of the cloud responses to aerosol changes[18,19] and the natural aerosol state that is being perturbed by anthropogenic emissions[14]. These prompt the need for both long term and *comprehensive* observations to understand key aerosol and cloud properties, and their controlling processes, for better representations in climate models.

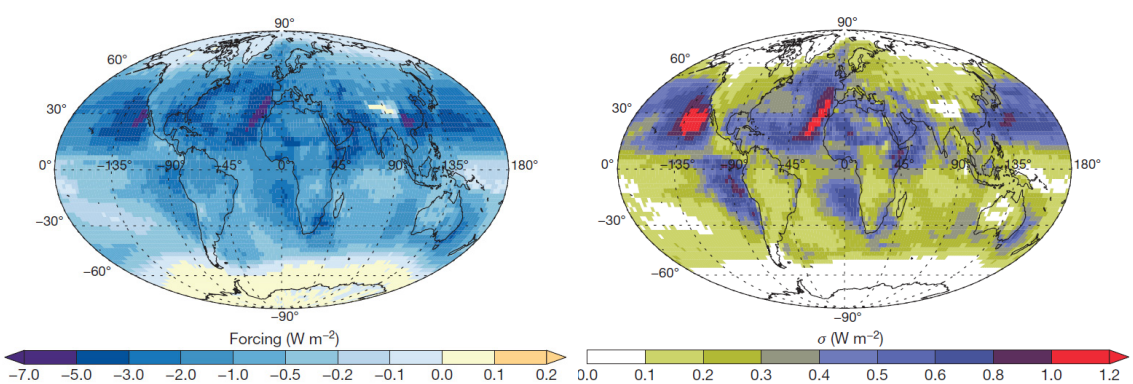

Figure 1. (a) Annual mean aerosol first indirect forcing, and (b) uncertainty in simulated first indirect forcing due to uncertainty in model (GLOMAP) parameters. Note the large aerosol indirect forcing and uncertainty in the ENA. Adapted from Carslaw et al.[14]

1.1.1 New Ground-Based, Long-Term Measurements at the ENA Site

The new Atmospheric Radiation Measurement (ARM) Eastern North Atlantic (ENA) site at Graciosa Island (The Azores, 28°W, 39°N) provides unprecedented observations in a remote marine environment dominated by low clouds (Figure 2). The ENA site greatly extends the capabilities of observational data sets collected as part of the Clouds-Aerosols-Precipitation Marine Boundary Layer (CAP-MBL) ARM Mobile Facility (AMF) deployment that took place in 2009-2010. The site straddles the boundary between the subtropics and mid-latitudes in the Eastern North Atlantic, and experiences a great diversity of meteorological and cloud conditions (Figure 2). In addition, the ENA site is downwind of the North American continent and is periodically impacted by continental anthropogenic aerosol[20,21]. The ENA site is thus in an excellent location to study the cloud condensation nuclei (CCN) budget in a remote marine region periodically perturbed by anthropogenic aerosols, and to investigate the impacts of long-range transport of aerosols on remote marine clouds.

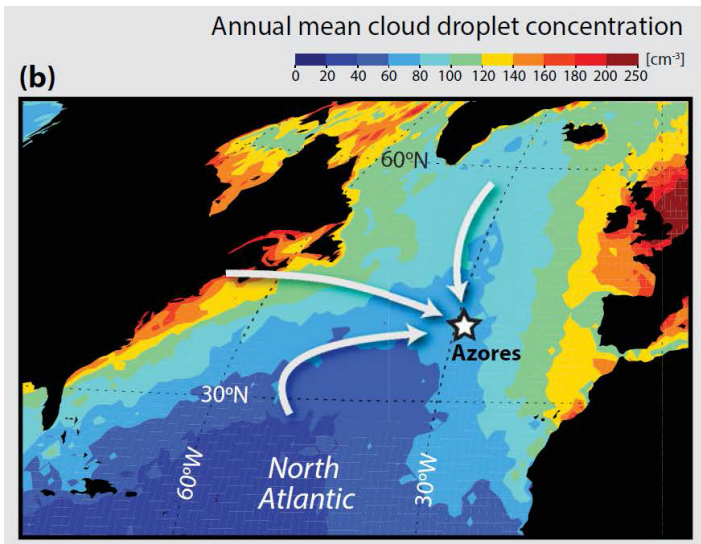

Figure 2. Map showing the location of the Azores in the Eastern North Atlantic. Colors show the annual-mean cloud droplet concentration for warm, overcast clouds as observed by the Moderate Resolution Imaging Spectroradiometer (MODIS) on the National Aeronautics and Space Administration (NASA) Terra satellite. The Azores receives a diverse range of air masses from North America, from the Arctic, and from northern Europe. Adapted from Wood et al.[20]

1.1.2 Budget of MBL CCN and its Seasonal Variation

The ENA site is influenced by a wide variety of air masses[22] and aerosol sources[20]. Cloud condensation nucleus concentrations in the ENA marine boundary layer (MBL) are substantially perturbed by anthropogenic emissions[21]. Figure 3 shows the major sources of boundary-layer CCN in a remote marine environment such as the ENA[23]. As a result of large-scale subsidence, the MBL in ENA is continually being modified by air entrained from the free troposphere (FT) with a timescale of several days. The sources of the FT aerosol include long-range transport of continental emissions, and particles produced via nucleation and new particle formation (NPF) in the outflow regions of distant deep convection[24]. Some of the FT aerosol particles are sufficiently large to serve as CCN when entrained[25,26], while others may grow into CCN through condensational growth in MBL[23,27,28] or through aqueous-phase processing

after activation in an anomalously strong updraft. NPF in the MBL may be infrequent and has mostly been observed when the pre-existing aerosol surface area was low under the conditions of low wind and/or heavy precipitation associated with open cell structure[29-31]. Kazil et al.[32] suggest that a nucleation source of aerosol in open cells may exceed sea salt emissions in terms of the number of particles produced. However, the impact of MBL NPF on CCN and marine low clouds remains poorly understood.

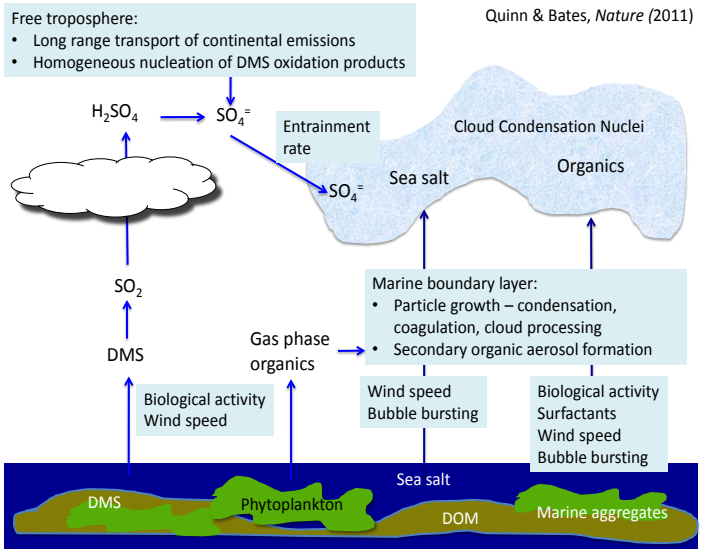

Figure 3. Major sources of boundary-layer CCN in a remote marine environment such as the ENA. Courtesy of Patricia Quinn.

Previous studies suggest entrainment from the FT may be the dominant source of CCN in the MBL[26,34]. Strong variations in CCN concentration were observed at the ENA site from April, 2009 to December, 2010 during CAP-MBL (Figure 4)[20]. Some of the high CCN concentration events are readily attributed to pollution transport from industrialized regions of North America, but some events may also be attributable to summertime biomass burning from the boreal forests of North America. The seasonal cycles of both CCN concentration and submicron aerosol scattering exhibit a spring/summer maximum and a minimum during winter, consistent with the spring maximum in CO observed at the nearby Pico Mountain Observatory on Pico Island, Azores (Figure 4). The maximum of CCN concentration and aerosol submicron aerosol scattering is likely due to more frequent transport from continental areas during the spring months[20], although stronger aerosol sink processes during wintertime may also contribute to the seasonality[35].

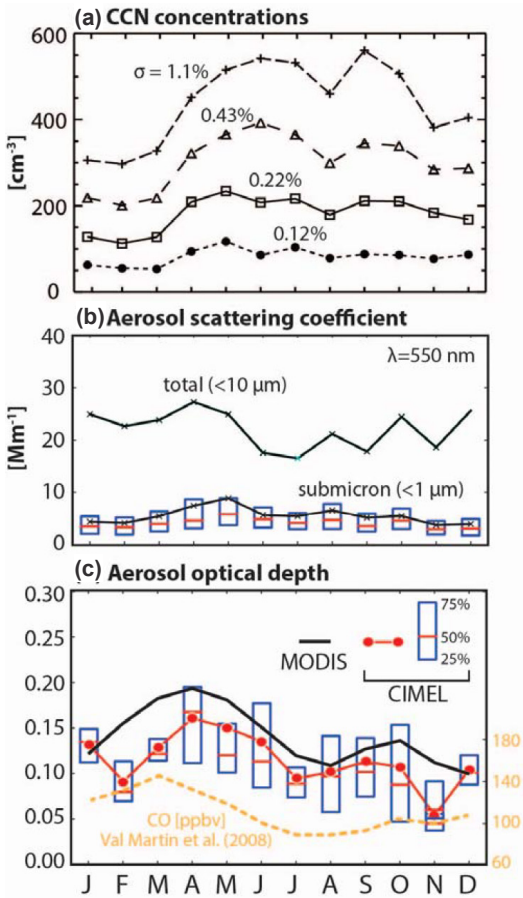

Figure 4. Composite seasonal cycles of (a) Surface CCN concentrations at four supersaturations. (b) Aerosol total and submicron dry extinction. Boxes span the 25th and 75th percentiles of the data with red bars indicating medians and the crosses indicating means. (c) Monthly-mean aerosol optical depth and 25th, 50th, and 75th percentile values from the Cimel sun photometer (red) and mean values from MODIS (black). The composite seasonal cycle of carbon monoxide measured at the Pico Mountain Observatory from 2002 to 2005 is also shown (see Val Martin et al.[33]).

Besides aerosol entrainment from the FT, sea spray aerosol (SSA) could also contribute significantly to the MBL CCN population. The sea spray aerosol particles are enriched in organic matter relative to seawater, especially in particles with diameter smaller than ~500 nm [36]. The presence of a large fraction of organic species in SSA particle may strongly impact their CCN activity and therefore interactions with marine clouds[37,38]. The organic sea spray fraction has been related to marine biological productivity through proxies such as chlorophyll-a (Chl-*a*) concentration[39]. However, Chl-*a* makes up only a very small fraction of the available organic matter, and this fraction can vary significantly among locations and seasons with different biological activities[40]. Therefore, a single relationship applicable across all ocean regions and different seasons between such proxies and the organic sea spray fraction remains elusive.

In the MBL, the main loss mechanism for CCN is coalescence scavenging, namely the process of drizzle drops accreting cloud droplets[26,41-43]. For example, over the southeastern Pacific Ocean, a large fraction of the observed geographical variability in cloud droplet concentration in extensive marine low clouds is driven by precipitation losses rather than aerosol source variability[26]. The loss by coalescence scavenging

likely depends on the mesoscale structure of low clouds. During CAP-MBL, events with very low CCN concentrations were often associated with extensive cold air outbreak air masses containing shallow open cell convection[44]. During VAMOS Ocean-Cloud-Atmosphere-Land Study Regional Experiment (VOCALS-REx), much lower accumulation mode aerosol concentrations were observed in the sub-cloud surface mixed layer of open cell regions compared with neighboring overcast regions, suggesting more efficient removal in open cells (Figure 5)[31]. The stratiform clouds in the open cells existed within a 200-300-m-thick ultra-clean layer with accumulation mode particle concentration as low as 0.1–1 cm^{-3}. This suggests that coalescence scavenging and sedimentation can in some cases be extremely efficient[31,45], as accumulation mode particle concentrations in the surface mixed layer, and droplet concentration in the active cumuli, were typically 20–60 cm^{-3}.

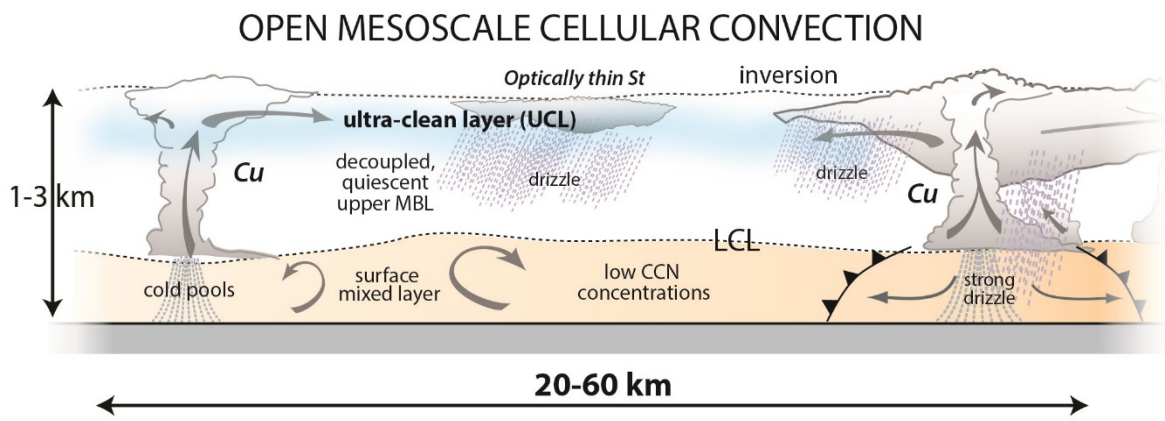

Figure 5. Diagram of open mesoscale cellular convection structure with an ultra-clean aerosol layer towards the top of the boundary layer.

While previous studies and routine measurements at the ENA site have provided invaluable information that aids in advancing our understanding of the aerosol budget in the remote MBL, we are far from achieving a quantitative understanding of the controlling processes sufficient to serve as a reliable foundation for developing GCM parameterizations and representations that will adequately simulate aerosol in past, current, and future climate. Some of the processes (e.g., MBL nucleation and its impact on CCN budget) remain poorly understood. Understanding and quantifying these key processes require comprehensive, multi-dimensional (e.g., size spectrum, chemical composition, mixing state, etc.) characterization of aerosol particles and trace gas precursors, and their vertical structure and mesoscale variability, which can be obtained only through aircraft-based measurements.

1.1.3 Effects of Aerosol on Clouds and Precipitation

Aerosols influence low clouds by changing the cloud droplet concentration (N_d), which impacts the cloud optical thickness even in the absence of cloud macrophysical changes[13]. These responses have been observed using ground-based and airborne sensors[46,47]. However, changing N_d also modifies the cloud droplet size and therefore the efficiency of precipitation formation[10], which can alter the macrophysical properties of low clouds. In the last decade, numerous field observations and modeling studies have confirmed that drizzle is strongly susceptible to N_d and CCN variations[48-51], including at the Azores[52], but cloud responses to drizzle suppression are complex and challenging to observe.

Suppression of drizzle by anthropogenic aerosols allows clouds to retain more condensate, which might lead to further increase in cloud albedo[10]. However, drizzle suppression also drives stronger turbulence and entrainment of free tropospheric air[53,54]. Aircraft observations of ship tracks[55] confirm earlier satellite studies (e.g., Coakley and Walsh[56]) in showing that cloud condensate responses to CCN increases can be positive and negative, and depend upon several aspects of the cloud state being perturbed, including cloud base height[54,57] and the dryness of the free troposphere[53,58].

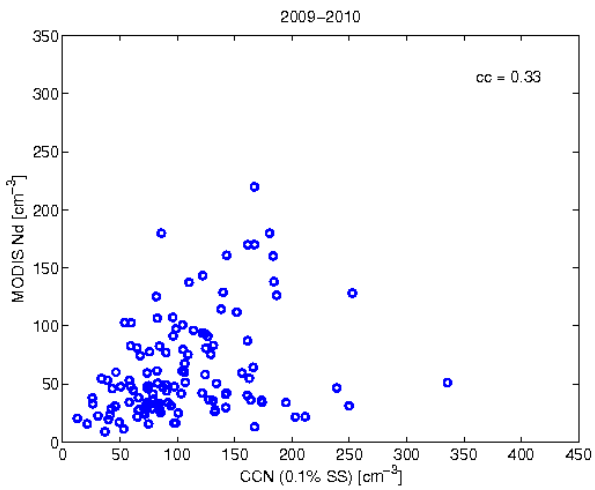

Figure 6. Cloud droplet concentration from the MODIS satellite plotted as a function of CCN concentration (0.1% supersaturation) measured on Graciosa during the CAP-MBL deployment (2009-2010). The correlation coefficient (i.e., R for a linear fit) is 0.33.

The MBL in the Azores is frequently *decoupled*[59], meaning that it comprises a two-layer structure with a surface mixed layer in contact with the ocean surface and a cloud-containing layer above that exhibits relatively slow (typically 12-24 hours[60]) exchange with the surface layer air and the free troposphere. Because the key MBL aerosol sources are a) the ocean surface and b) entrainment from the free troposphere[26], the cloud layer may not experience the same aerosol conditions as the near-surface air under the frequent decoupled MBL condition. To aid the interpretation of the long-term ENA surface aerosol measurements, we need to better understand and quantify the connection between the properties of CCN measured at the surface and at the cloud base. Over the subtropical NE Pacific, shipborne CCN measurements from the Marine ARM GPCI (GCSS [GEWEX {Global Energy and Water Cycle Experiment}Cloud Systems Study] Pacific Cross-Section Intercomparison) Investigation of Clouds (MAGIC) campaign combined with N_d estimates from satellites reveal very different sensitivities of N_d to CCN concentrations when the MBL is coupled and decoupled[61]. At the ENA site, as is typical of the mid-latitude oceans[62], the greater prevalence of decoupled vs. coupled MBLs suggests that the coupling between surface and cloud base CCN might be weak (Figure 6 and Fig. 6 in Dong et al.[63]), but systematic airborne observations are needed to ascertain this and also to identify how ground-based lidar and CCN measurements may be used to better infer the CCN concentrations at cloud base.

Airborne measurements during the Atlantic Stratocumulus Transition Experiment (ASTEX) in 1992 indicate that there is considerable variability in CCN and N_d in the Azores[25], and that N_d values are strongly related to accumulation mode aerosol concentrations (N_a) just below cloud base (Figure 7). As

expected, the slope of the relationship is strongest at low aerosol loading, consistent with expectations from condensational growth[65,66]. The variation in the slope of N_d vs. N_a suggests different regimes for droplet activation (e.g., aerosol-limited to updraft-limited). The tight coupling exhibited from aircraft-based measurements implies potential anthropogenic impacts that may not be captured using metrics based on surface CCN measurements.

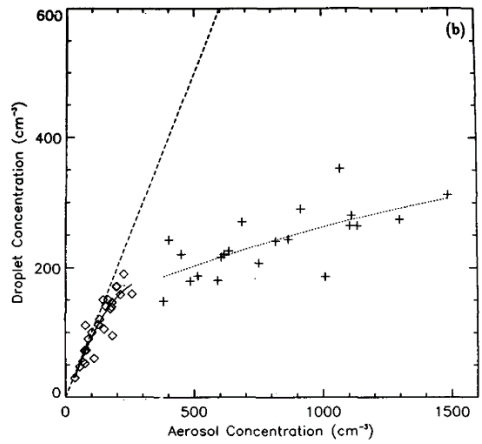

Figure 7. Cloud droplet concentration plotted as a function of cloud base aerosol concentration (particles > 0.1 micron size) for measurements during summer 1992 during ASTEX in the vicinity of the Azores. Diamonds are cases without significant continental aerosol, and crosses are continentally influenced. From Martin et al.[64]

Understanding the effects of aerosol-driven N_d variability on cloud optical properties and precipitation was not a primary focus during ASTEX and new measurement techniques can provide new insights into the relationships between CCN, cloud droplet concentrations, precipitation microphysical properties, and cloud macro-scale structure. In addition, the sampling during ASTEX was only during summer, but the knowledge of the seasonal cycle of CCN, its contributing sources and sinks, and the seasonally varying MBL decoupling is critical for understanding aerosol impacts on cloud microphysical and macrophysical properties. Improved understanding of the CCN budget, especially the contributions from FT long-range transported aerosols and from the ocean surface, will allow us to better relate cloud base CCN, and therefore N_d, to the various sources.

Observations of the sensitivity of light precipitation to CCN and N_d variability have largely used measurements in shallower, better-mixed MBLs than are typically observed in the ENA. Precipitating structures at ENA range from stratocumulus with virga to quite deep (few km) open cell convection with relatively large precipitating cells. It is likely that aerosols impact the precipitation falling from these different cloud types in different ways, with precipitation from deeper clouds likely being less sensitive to aerosol changes than precipitation from shallow ones[51,67], although different precipitation susceptibility studies disagree on this point[50,68]. Satellites tend to show relatively weak dependence of precipitation on aerosols[69], and these measurements have been used to constrain LWP responses to anthropogenic aerosol[70]. However, other studies show that light precipitation is quite strongly sensitive to N_d [68,71], leaving a significant knowledge gap that has major impacts on the magnitude of aerosol indirect effects.

1.1.4 Cloud Microphysical and Macrophysical Structures, and Entrainment Mixing

As described above, the impact of aerosol on precipitation depends on both microphysical and macrophysical structure of clouds. Improved understanding of precipitating low cloud systems under a broader range of meteorological and cloudiness conditions is clearly needed to understand their sensitivity to meteorology and to aerosols. Model simulations show that the balance of microphysical process rates, in particular the ratio of autoconversion to accretion, is important for understanding precipitation susceptibility to aerosol[71,72]. In addition, as collision-coalescence of cloud droplets is the primary loss mechanism for CCN in the MBL[26,43], understanding of the MBL CCN budget necessitates the quantification of the microphysical process rates. Cloud microphysical measurements onboard aircraft have been used to partition condensate into cloud and precipitation hydrometeors and to derive microphysical process rates[72-74]. However, no study has been able to combine aircraft measurements in marine low clouds with collocated high-sensitivity, scanning radar data to explore how the process rates vary across precipitating cloud systems and vary with the type of mesoscale organization. Observations from previous aircraft campaigns in closed cell stratocumulus show strong correlations between liquid water content and cloud droplet concentration on the mesoscale. It is not clear whether these correlations are caused by updraft variability or are a sign of coalescence scavenging of cloud drops. Measurements from VOCALS-REx[31] hint that as the mesoscale cells age over a typical lifetime of 1-2 hours[75], they become far more drizzle-rich and their turbulence subsides. Again, these mesoscale structures and evolutions of clouds are poorly understood in part because of a lack of scanning radar to place the microphysical measurements into a cloud mesoscale and lifecycle context.

Satellite observations with NASA's CloudSat mission indicate considerable differences in the shape of the precipitation distribution for different types of mesoscale cellular convection[77], but CloudSat has problems with ground clutter and vertical resolution that are alleviated with the new radars at the ENA site. The spatial distribution of precipitation from the X-band scanning ARM precipitation radar (new XSAPR2) will provide much greater statistical sampling than single-point measurements alone (see Figure 8 for an example showing C-band radar from MBL clouds over the southeastern Pacific during the East Pacific Investigation of Climate). The XSAPR2 is a one-of-a-kind X-band radar with: i) sufficient sensitivity (-20 dBZ at 40 km range) ii) narrow beamwidth (0.5°) to maintain reasonable vertical and horizontal resolution at long ranges (250 m at 30 km), and iii) polarization diversity to facilitate the removal of sea clutter (Kollias, personal communication). The XSAPR2 is expected to provide cloud-base and subcloud-layer drizzle rates, and in situ measurements away from the island will be critical for evaluation of the drizzle retrieval algorithm currently under development.

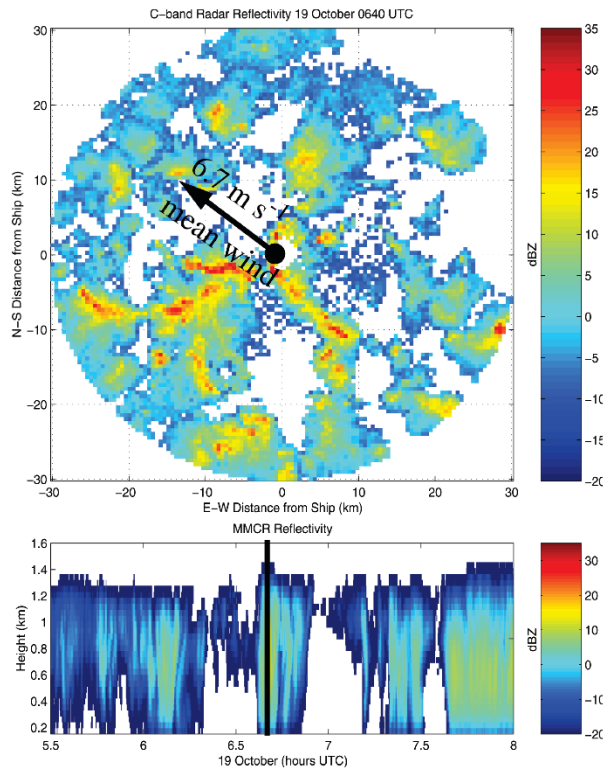

Figure 8. Horizontal cross section of 5-cm radar reflectivity at 1-km elevation during a heavy drizzle period (ship location at black dot, arrow shows MBL wind direction) and (bottom) time–height plot of 8-mm radar reflectivity above the ship (black line shows time of upper image) during the East Pacific Investigation of Climate (EPIC) 2001 study. Adapted from Bretherton et al.[76]

The entrainment of free tropospheric air into the cloud-topped marine boundary layer has important consequences for the thermodynamic structure as well as cloud macro- and microphysical properties. Direct, non-turbulent mixing results in a deepening of the boundary layer[78], eventually leading to a decoupling of the surface and cloud layers when cloud-top longwave cooling can no longer sustain mixing through the depth of the boundary layer[79]. Turbulent mixing results in evaporation of cloud droplets and subsequent deviations from adiabatic liquid water profiles[80,81]. These effects further combine to control the macrophysical structure of MBL clouds. The magnitude of cloud-top entrainment is driven by the strength of gradients in buoyancy and horizontal winds in the Entrainment Interfacial Layer (EIL)[82-84]; however, the details of how the entrainment rate relates to the turbulent dynamics of the boundary layer remains one of the main unresolved questions of MBL dynamics. Equally important, yet poorly understood, are the subsequent turbulent mixing processes and their effects on cloud microphysics[85,86]. For example, model sensitivity studies have demonstrated that the assumed entrainment mixing process (e.g., extreme homogeneous or inhomogeneous entrainment mixing) can significantly impact cloud microphysical properties, cloud radiative properties, and aerosol indirect effects[87,88]. However, it is unclear whether the mixing process is predominantly homogeneous, inhomogeneous, or in between; what factors control the mixing process; and how they interact[89]. The intimate connections among the microphysical, dynamical, and thermodynamic properties associated with different entrainment-mixing processes remains poorly understood[85,90,91]. Advances in measurement techniques can provide new insights into and help quantify entrainment-mixing processes and their microphysical-

dynamical-thermodynamic connections for improved representations of entrainment mixing processes and their microphysical effects in models.

1.1.5 Advancing Retrievals of Turbulence, Clouds, and Drizzle

While ARM's longstanding observations have proved invaluable in advancing our understanding of cloud properties and associated processes, the lack of capability to observe precipitating clouds and to capture 3D cloud structures is well recognized and needs to be addressed. The ENA site is equipped with state-of-the-art profiling and scanning radars and lidars along with passive microwave and shortwave observation sensors. The availability of these sensors at multiple wavelengths provides the opportunity to employ state-of-the-art retrieval algorithms for turbulence, cloud, and drizzle. Despite their sophistication, these retrievals techniques are in need of extensive validation.

Comprehensive in situ measurements are essential for validating and advancing ARM remote-sensing techniques for clouds in three aspects. First, drizzle below clouds is an important variable for quantifying aerosol impacts on precipitation, and for investigating drizzle impacts on the thermodynamics and dynamics in sub-cloud layers. Perhaps the area/type of retrieval in which we have the most confidence is drizzle properties (flux, and particle size distribution) below the cloud base due to availability of lidar measurements. Current state-of-the-art techniques for retrieving drizzle below clouds mainly exploit a combination of radar only[92], lidar and radar[93,94], or differences in backscatter at two different lidar wavelengths[95]. However, preliminary intercomparisons between retrievals have shown considerable differences, and these techniques need to be evaluated for the particular ENA climatology.

Retrieving drizzle properties above the cloud base is far more challenging due to the lack of lidar measurements above the cloud base. It is also of great importance to know the properties of cloud droplets (e.g., water content, effective radius). A number of methods have been proposed, including separating cloud and drizzle signatures from Doppler spectra[96,97] and subtracting the cloud signature that is inferred from shortwave radiances from the total radar reflectivity[98]. Up to now, no intercomparison between these methods has been performed. In addition to cloud and drizzle properties, the availability of Doppler velocity measurements from the profiling radars and lidars provides us with the opportunity of seamless dynamical retrievals of vertical air motion and eddy dissipation rates below and above the cloud base, independent of the presence or not of drizzle particles[99]. In situ turbulence measurements over a wide range of conditions are needed to evaluate the new dynamical retrievals.

The ARM new scanning radar measurements provide exciting opportunities for volumetric retrievals of hydrometeor locations and properties[100,101]. Lamer et al.[102] developed gridded fields from the Scanning ARM Cloud Radars (SACRs) and a technique for retrieving 3D vertical velocity from SACR measurements. Fielding et al.[103] developed a novel ENsemble ClOud REtrieval (ENCORE) method to provide 3D fields of cloud water content and droplet size in both overcast and broken cloud conditions (see Figure 9 for examples from the AMF deployment at the Azores). Because ARM passive instruments have difficulty capturing cumulus due to its low water path and highly heterogeneous structure, this example highlights how the new scanning radars can greatly enhance cumulus observations and will help provide detailed sub-grid variability and organization of clouds, giving insight into the 3D radiative properties of boundary-layer clouds.

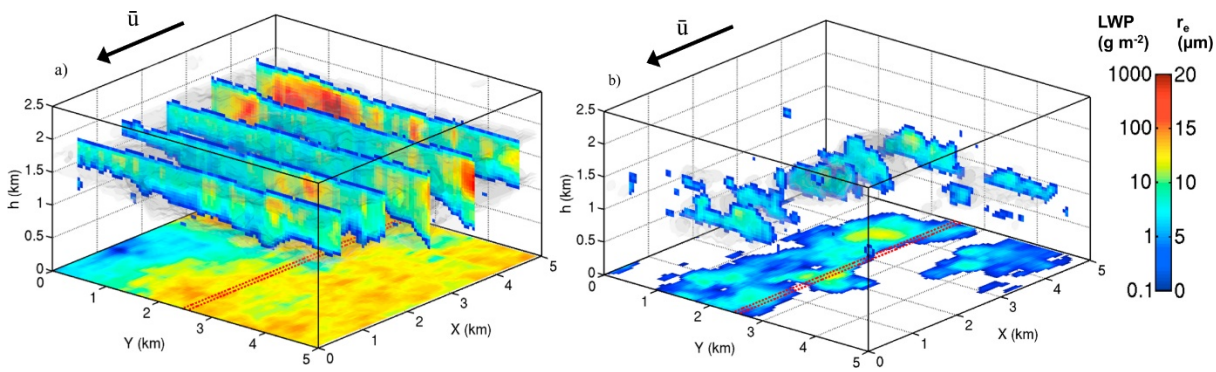

Figure 9. Retrieved cloud fields for (left) stratocumulus case and (right) cumulus case, with 3D liquid water content plotted as grey isosurfaces, slices of 3D effective radius (r_e) plotted along the Y axis and liquid water path (LWP) plotted at the surface. The mean wind (u) direction is shown by the black arrow, while the track of radiances along Y = 2.5 km is shown by the red dashed line.

All the aforementioned retrieval methods involve certain assumptions regarding size distributions and/or cloud vertical profiles, which were supported by limited sets of simulations and past field campaigns but have not been thoroughly compared against each other as a whole. A comprehensive intercomparison at the ENA site will evaluate how well these assumptions work in various cloud regimes and, more importantly, provide guidelines and recommendations for users. Estimating the true uncertainty in a retrieval method is difficult; intercomparison against in situ aircraft measurements will also help evaluate whether the retrieval uncertainty has been appropriately estimated.

1.2 Scientific Objectives

The ACE-ENA campaign is motivated by the need for comprehensive in situ characterizations of boundary-layer and lower FT structure, and associated vertical distributions and horizontal variabilities of low clouds and aerosol over the Azores. The overarching scientific objective is to understand key processes that drive the properties and interactions of aerosol and cloud under a variety of representative meteorological and cloud conditions. An important consideration for this deployment is to provide high-quality in situ measurements for validating and improving ground-based retrieval algorithms at the ENA site. This will lead to high-quality, long-term data sets from the routine ground-based remote sensing, which will allow greater statistical reliability in the observed properties and relationships among aerosols, clouds, and precipitation than is possible with the aircraft measurements alone. The in situ data and improved algorithms will enable better use of the routine measurements for model evaluation. Scientific questions and objectives, organized into five themes, are:

- <u>Budget of MBL CCN and its Seasonal Variation</u>
    - What are the contributions from different sources, including sea spray aerosol, long-range transport, and new particle formation? What are the seasonal variations of the characteristics and contributions of various sources?
    - How does removal of CCN by droplet coalescence control the CCN population in the MBL for representative cloud regimes?

- Effects of Aerosol on Clouds and Precipitation
    - How can ground-based lidar and CCN measurements be used to better infer CCN concentration at cloud base?
    - How does the CCN budget affect cloud microphysics? Do high CCN concentrations lead to increased cloud droplet concentrations and suppressed precipitation? Is precipitation susceptibility to CCN weaker in the deep open cells observed in the Azores?
- Cloud Microphysical and Macrophysical Structures, and Entrainment Mixing
    - What are the mesoscale variabilities of cloud microphysics and vertical velocity and how do they influence drizzle mesoscale organization and rates? What are the thermodynamic and spatial characteristics of cold pools and how do they relate to the properties and mesoscale organizations of cloud and drizzle?
    - What are the relationships between the entrainment rate, thermodynamic stability, wind shear above cloud top, and coupling structure below cloud base? What is the prevalent entrainment mixing mechanism, and what are the controlling factors? What are the microphysical effects of entrainment mixing?
- Advancing Retrievals of Turbulence, Cloud, and Drizzle
    - Validating and quantifying the uncertainties in turbulence, cloud and drizzle microphysical properties retrieved from vertically pointing observations
    - Validating and improving 3D cloud and drizzle retrievals from scanning radars
- Model Evaluation and Processes Studies
    - Comparison of the airborne data with predictions of global models using “nudged” or “specified” meteorology and local simulations with LES and WRF-Chem models.
    - Examining the CCN budget terms and processes driving the vertical structure and mesoscale variation of aerosol, cloud, and drizzle fields using validated/constrained GCM and LES model simulations.

1.3 Deployment Strategies

Simultaneous characterizations of meteorological parameters, trace gases, aerosol, cloud, and drizzle fields will be carried out onboard the ARM Aerial Facility Gulfstream-1 (G-1) aircraft near the ENA site. The campaign will consist of two Intensive Operational Periods (IOPs), one during early summer from June to July 2017, and the second one from January to February 2018 during the winter season. Deployments during both seasons allow for examination of key aerosol and cloud processes under a variety of representative meteorological and cloud conditions, and for different aerosol sources and pathways. For example, during the summer months, the Azores are ideally located to sample overcast stratocumulus, and the transition to a broken trade cumulus regime; the winter frequently experiences maritime frontal clouds. The CCN population during the winter is likely dominated by sea spray aerosol. In the summer season, sea spray aerosol is enriched in primary organic species, and the entrainment of biogenically derived aerosols and longer-range transported continental pollution is likely a major source of CCN in the boundary layer.

A key advantage of the deployments is the strong synergy between the in situ measurements onboard the G-1 and the ongoing measurements at the ENA site, including state-of-the-art profiling and scanning radars. The 3D cloud structures provided by the scanning radars will put the detailed in situ measurements into mesoscale and cloud lifecycle contexts. On the other hand, high-quality in situ measurements will enable validation and improvements of ground-based retrieval algorithms at the ENA site, leading to high-quality, statistically robust data sets from the routine measurements. The ACE-ENA deployments, combined with the ongoing measurements at the ENA site, will have a long-lasting impact on the research and modeling of clouds and aerosols in remote marine environments.

1.3.1 Instruments and Measurements Onboard G-1

A list of the instruments and measurements is included in Section 6. Measurements onboard the G-1 will include the standard meteorological, turbulence, and radiation (both up and downwelling) quantities, including measurements of sensible and latent heat fluxes. The size distribution of cloud droplets, drizzle, and rain drops will be characterized using a combination of Fast Cloud Droplet probe (FCDP), 2-Dimensional Stereo Probe (2D-S), and High-Volume Precipitation Spectrometer Version 3 (HVPS-3). Liquid water content will be measured using both a Multi-Element Water Content System (WCM-2000) and a Gerber (PVM-100a) probe. We also plan to deploy a Cloud, Aerosol, and Precipitation Spectrometer (CAPS) that will provide redundant measurements of cloud droplet and drizzle drop size spectra and liquid water content. A novel Holographic Detector for Clouds (HOLODEC) will be deployed to sample an ensemble of hydrometeors in a localized volume (~ 20 cm^3) by digitally reconstructing interference patterns recorded by a charge-coupled device (CCD) camera[104]. Under typical stratocumulus conditions, each sampled region of cloud will result in a statistically robust estimate of the cloud droplet size distribution, without the loss of information inherent in averaging over long distances.

Trace gas monitors that measure carbon monoxide (CO) and ozone (O_3) will help differentiate various air masses and identify the influences from anthropogenic emissions. A Proton Transfer Reaction-Mass Spectrometer (PTR-MS) will characterize important trace gas volatile organic compounds (VOCs), including key aerosol precursors and relevant reaction products. Comprehensive characterizations of aerosol include particle number concentration, size distribution, optical properties, and chemical composition. A Fast Integrated Mobility Spectrometer (FIMS), Ultra-High Sensitivity Aerosol Spectrometer (UHSAS), Passive Cavity Aerosol Spectrometer (PCASP), and Cloud and Aerosol Spectrometer (CAS, part of the CAPS) provide size distribution from 10-nm to coarse-size particles. A Condensation Particle Counter (CPC) (for sizes > 10 nm) and an Ultrafine Condensation Particle Counter (UCPC) (for sizes > 3 nm) will quantify total aerosol number concentrations. A Single Particle Soot Photometer (SP2) will be used to measure refractory black carbon concentrations, a High-Resolution Time-of-Flight Aerosol Mass Spectrometer (HR-ToF-AMS) will characterize bulk aerosol composition and size, and a Particle-Into-Liquid Sampler (PILS) coupled to ion chromatography will characterize sub-micrometer water-soluble aerosol chemical composition (i.e., inorganics, organic acids, amines). A TRAC sampler will be deployed to collect atmospheric particles for multiple off-line, post-campaign, laboratory analyses[105,106]. Optical properties for aerosol absorption and scattering will be measured by a Particle Soot Absorption Photometer (PSAP) and nephelometer, respectively. A dual-column CCN counter will be used to quantify cloud condensation nuclei concentrations.

Aerosol size distribution measured by the FIMS and total number concentration measurements will alternate between ambient samples and those processed by a thermal denuder, which allows volatility-

based separation by exploiting the higher volatility of organics and sulfate versus sea salt and refractory black carbon[34], which remain in the aerosol phase at the denuder temperature of 350 °C. We also plan to use both an isokinetic inlet and a counter-flow virtual impactor (CVI) inlet to sample aerosols, similar to the previous G-1 deployments (e.g., the Two-Column Aerosol Project [TCAP] and the ARM Cloud Aerosol Precipitation Experiment [ACAPEX]). When used to sample cloud droplets, the CVI allows determination of particle composition and size spectrum of cloud droplet residuals by the HR-ToF-AMS, PILS, SP2, and FIMS.

The measurements of meteorological parameters, cloud microphysics, and aerosol number concentration and size distribution will be carried out at a frequency of 1 Hz or higher. Cloud droplet spectrum will be measured by the FCDP at a frequency of 10 Hz. In addition, both FCDP and UHSAS have the "particle by particle" sampling capability, therefore allowing measurements at even higher frequency. The Gerber probe will be operated at a frequency of 100 Hz. These high-resolution cloud microphysics measurements, combined with the unique data set provided by the HOLODEC, will be critical for understanding and quantifying the microphysical impact of the entrainment mixing processes.

1.3.2 Flight Plans

The basic flight patterns will include spirals to obtain vertical profiles of aerosol and clouds, and legs at multiple altitudes, including below cloud, inside cloud, at the cloud top, and in the free troposphere. Each leg will be several tens of kilometers in length to capture the mesoscale variabilities of aerosol and cloud fields. The legs will tend to be flown either perpendicular to or along the wind direction. These measurements will provide detailed characterization of boundary-layer and lower FT structure, and associated vertical distributions and horizontal variations of low clouds and aerosols in the Azores under representative meteorological and cloud conditions. The G-1 may be stationed at the Lajes airport on the island of Terceira, which is about 90 km from the ENA site. There will be 80 flight hours during each IOP, corresponding to approximately 20 four-hour flights. The preliminary flight plans are described below.

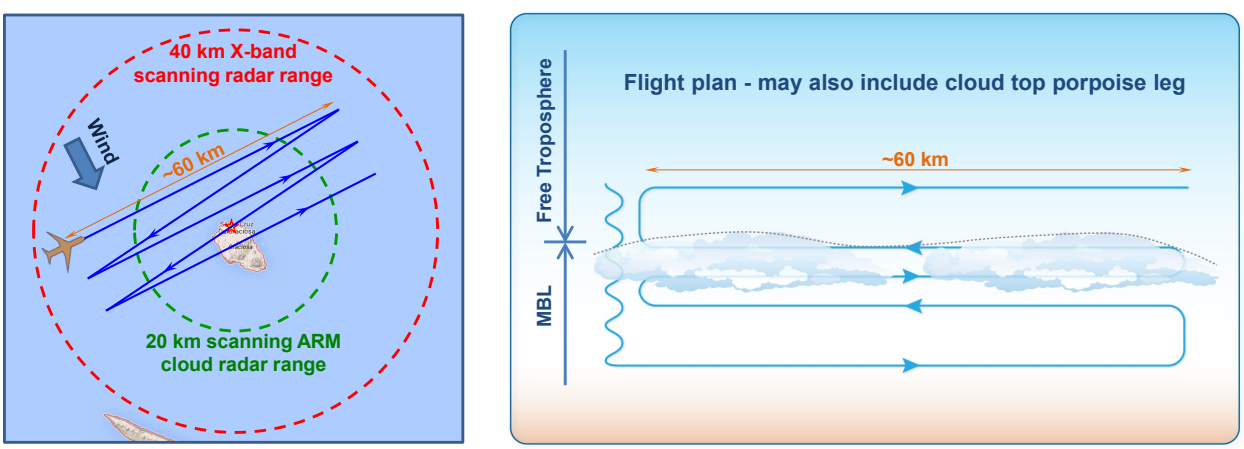

Figure 10. Flight plan for characterizing the vertical structure and mesoscale variation of thermodynamics, aerosol, cloud, and precipitation.

1.3.2.1 Lagrangian Drift for Characterizing the Vertical Structure and Mesoscale Variation of Thermodynamics, Aerosol, Cloud, and Precipitation

This flight plan is designed to study key cloud and aerosol-controlling processes in representative cloud regimes. The G-1 will start at a location ~ 20 km upwind of the ENA site (Figure 10). Following a spiral to profile the MBL and lower FT vertical structure, the G-1 will perform across-wind stacks of five straight and level runs approximately 60 km in length below, in, and above cloud (with additional porpoising runs to characterize the cloud top and inversion layers). The aircraft will be allowed to drift with the MBL mean wind towards the ENA site. The total time for the first four stacked levels within the MBL is estimated to be 45 minutes. Figure 10 shows an example of flight tracks with an average MBL wind speed of 20 km/hour. The fourth-level run will pass over the ENA site, facilitating the comparison of in situ measurements with the retrievals from vertically pointing observations. Under this typical wind speed, most of the G-1 flight tracks are within the 20 km scanning ARM cloud radar (SACR2) range for cloud and drizzle retrievals and all flight tracks are within the 40 km X-band scanning ARM precipitation radar (XSAPR2) range for drizzle retrieval. The G-1 will start with lower-level runs (further away from the site) to take advantage of the longer range of the XSAPR2. The flight pattern will be adjusted according to the wind direction and speed. For example, under light wind conditions additional levels (e.g., porpoising runs at cloud top) will be included. The flight will be coordinated with SACR2 and XSAPR2 operations in consultation with the radar mentors and ARM Radar operations committee, and a combination of scanning modes, including upwind boundary layer Range Height Indicator (RHI), crosswind RHI, and downwind boundary layer RHI will be used to provide the mesoscale and cloud lifetime contexts for the in situ sampling onboard the G-1. We will also explore the possibility of using available real-time G-1 position to further control the scanning radar's azimuth during scans. The flight pattern will be repeated for different cloud regimes during the IOPs, including overcast stratocumulus, the transition to broken trade cumulus regime, and maritime frontal clouds. A second "drift" flight plan (not shown) will involve repeated tight spirals. During these tight spirals, the G-1 will be allowed to drift with the mean MBL wind towards the ENA site, to provide detailed vertical structures of the same cloud and drizzle clusters and their evolution.

1.3.2.2 Validation of Retrievals from Vertically Pointing Observations

The G-1 will carry out repeated spirals near the ENA site and straight and level runs at multiple altitudes, approximately 20-30 km in length (i.e., within scanning cloud radar range) along the direction of the MBL wind between two fixed points, one over the land and the other upwind over the ocean. The level runs will be below, in, and above clouds and pass directly above the ENA site. This flight plan will provide comprehensive data sets that are essential for validating retrievals based on vertically pointing observations. Additional porpoising runs or level runs near cloud top will also be carried out to characterize the cloud top and inversion layers for studying turbulence and entrainment mixing. This flight plan will also allow us to examine the potential uncertainty in retrievals due to island effects, and the impact of wave-breaking at shoreline on aerosol CCN spectrum and optical properties measured at the ENA site. While the minimum sampling altitude over Graciosa Island is subject to aviation authority approval, our communications with AAF Director of Flight Operations suggest that the G-1 would likely be able to do sampling as low as ~150 m above the ground over the ENA site, therefore allowing characterization of drizzle below the cloud base, given the typical cloud base height observed in the Azores. We will also explore the possibility of profiling the boundary layer using "missed approaches" near the ENA site.

1.3.2.3 Additional Aerosol Profiling in FT

If time permits at the start or end of flights, we will also carry out a vertical profile up to 5000 m to identify potential elevated aerosol layers in the FT, which will then be sampled using horizontal legs.

Prior to the deployments, LES simulations will be carried out and the results will be used to optimize the sampling strategy and refine the flight patterns. We will work closely with AAF staff in finalizing flight paths, weighing the science objectives with the logistical considerations. During the IOPs, forecasting operations will use global forecast models such as the MACC (Monitoring Atmospheric Composition and Climate), GFS (Global Forecast System) and ECMWF (European Centre for Medium-Range Weather Forecasts) to make both short- and long-term predictions. These forecasts, combined with satellite images, will be used to aid daily decisions on flight plans.

1.3.3 Surface Measurements

We will supplement the routine measurements at the ENA site with a few measurements that are important for addressing the scientific objectives outlined above. Collectively, the routine and supplementary measurements provide important seasonal context for the G-1 sampling. These measurements include two additional soundings per day (total four per day) on days when G-1 is sampling. For a one-year period from May 2017 to April 2018, an Ultrafine Condensation Particle Counter (UCPC) will be deployed to quantify total number concentration of particles with diameter greater than 3 nm, a Scanning Mobility Particle Sizer (SMPS) will be used to characterize particle size distribution between diameters 10 and 500 nm, and size-resolved CCN spectrum will be characterized at the typical supersaturation range for marine low clouds. The combination of the UCPC and routine CPC measurement at the ENA site will yield information on MBL nucleation/new particle formation events. Similar to the size distribution measurement by the FIMS onboard the G-1, the SMPS measurement will alternate between ambient samples and those processed by a thermal denuder, which allows volatility-based separation of organics and sulfate from sea salt and soot. Size-resolved CCN spectrum will provide particle mixing state and hygroscopicity under supersaturated conditions pertinent to cloud droplet activation.

1.4 Synergistic Activities and Coordination with Other Studies

There will be strong synergies between the ACE-ENA deployments and a number of other field studies that will also take place in the ENA. The North Atlantic Aerosols and Marine Ecosystems Study (NAAMES), a NASA Earth Venture Suborbital (EVS) mission, will take place from 2015 to 2019. One of the main objectives of NAAMES is to understand how remote marine aerosols and boundary-layer clouds are influenced by plankton ecosystems in the North Atlantic. NAAMES consists of four deployments, including both ship- and aircraft-based measurements of trace gases, aerosols, and clouds, with likely sampling in the Azores. We will collaborate with Dr. Michael Behrenfeld (NAAMES PI) and Dr. Chris Hostetler (NAAMES Project Scientist and lead for the airborne component), and leverage the NAAMES measurements including those made during the two other seasons (e.g., spring and fall). Given its large spatial coverage, the measurements onboard the NASA P-3 aircraft could also provide spatial context for the G-1 deployment.

We will also collaborate with Dr. Holger Siebert from the Institute for Tropospheric Research in Leipzig, Germany, who is the PI for the helicopter-borne cloud-turbulence measurement system, ACTOS. A proposal has been submitted to the German NSF to bring ACTOS for a deployment in the Azores in summer months of 2017. ACTOS allows for high resolution and spatially collocated measurements of aerosol and cloud microphysics, turbulence, thermodynamics, and radiation. We plan to leverage the small spatial details provide by the Airborne Cloud Turbulence Observation System (ACTOS), including turbulence, thermodynamics, and cloud microphysics, and collaborate with Dr. Siebert to improve the understanding and quantification of entrainment rate and the impact of the entrainment mixing on cloud microphysics.

Measurements of atmospheric chemistry in the lower FT over the Azores are carried out at the Pico Mountain Observatory (PMO). The objective is to make direct measurements over the ENA of pollutants transported from North America and Europe, as well as characterization of pristine free-tropospheric air masses. The PMO, at the summit of Pico, is ideally located to sample intercontinental transport, which mostly occurs in the free troposphere. These measurements are used to determine the frequency and magnitude of transport events that disperse ozone and carbon monoxide. Additional measurements including aerosol optical properties were carried out and aerosol filters samples were collected from 2012 to 2014. We will collaborate with Dr. Claudio Mazzoleni of Michigan Technical University, who is leading the operation of the observatory, to leverage the measurements at the PMO for understanding the contribution of FT entrainment to boundary CCN population.

2.0 Scientific Objectives and Research

The overarching goal of ACE-ENA is to provide comprehensive in situ characterizations of boundary-layer and lower FT structure, and associated vertical distributions and horizontal variations of low clouds and aerosol in the Azores. This will allow in-depth understanding and quantification of key processes that drive the properties and interactions of aerosol, cloud, and precipitation under a variety of representative meteorological and cloud conditions. The scientific objectives and research are discussed below along five thematic lines. The impact of the deployments will go beyond the research activities outlined in this section, and will have a long-lasting impact on the research and modeling of clouds and aerosols in remote marine environments.

2.1 Budget of MBL CCN and its Seasonal Variation (Azevedo, Chand, Gilles, Jefferson, Kuang, Laskin, Lewis, McComiskey, Mei, Sedlacek, Wang, Wood)

2.1.1 Contributions from Different Sources and their Seasonal Variations

Given the high susceptibility of marine low cloud to perturbation in aerosol properties, the understanding of the aerosol budget in MBL and its controlling processes is critical for simulating aerosol indirect effects in present and future climate. One of the key challenges is to differentiate and quantify the contributions from different sources to MBL aerosol and CCN. The G-1 payload provides a number of complementary composition measurement techniques capable of distinguishing between major aerosol types, including sea spray aerosol, organic-sulfate mixture, and soot containing particles. These

techniques include volatility-based separation followed by size distribution and concentration measurements that exploit the higher volatility of organics and sulfate versus sea salt and refractory black carbon. Refractory black carbon mass concentration of individual particles is characterized by SP2. The combination of Aerosol Mass Spectrometer (AMS) and PILS captures the total and water soluble organics, sulfate, nitrate, and sea salt mass loadings. In addition, PILS also provides the concentration of organic acids, which are linked to cloud processing of aerosol particles. The detailed aerosol size spectrum will be used to identify particles produced via nucleation and new particle formation (i.e., as evident by an enhanced concentration of nucleation mode particles). Comprehensive offline analyses of collected particle samples will be carried out to characterize particle mixing state, morphology, and functional group (examples are shown in Figure 11). The trace gas measurements such as CO and ozone will help differentiate various air masses and identify the influences from anthropogenic emissions. The air mass analysis will be combined with back-trajectory simulations. Collectively, the multi-dimensional characterizations of aerosol particles, their vertical structure and mesoscale variations, and the information on air masses, will allow us to piece together a more complete picture of sampled particles, therefore allowing effective attribution to different sources and quantification of their contributions. The analyses will be carried out for representative meteorological and cloud conditions. The deployments during the two seasons also allow us to examine the seasonal variations of major aerosol sources and their contributions to MBL CCN population.

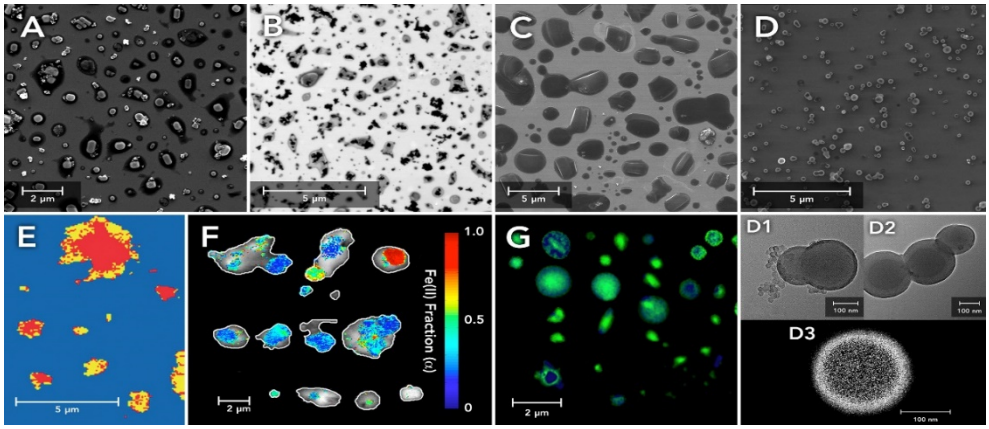

Figure 11. Electron microscopy (panels A-D) and X-ray spectromicroscopy (panels E-G) images illustrating morphology and the internal composition of particles from various sources collected in field studies. (Panel A) Inorganic particles coated with secondary organic material collected at ground site in Mexico City, Mexico[107]. (Panel B) Black carbon particles coated with secondary organic material collected at ground site in Los Angeles, California[108]. (Panel C) Internally mixed organic/sulfate particles apportioned to a power plant plume, sampled aboard G-1 aircraft during research flight in Massachusetts[109]. (Panel D) Primary emitted biomass-burning tar-ball particles collected at ground site in Yosemite National Park, California. Inserts 1-3 show magnified images of individual particles indicating internal chemical heterogeneity[110]. (Panel E) Marine particles collected at ground site in Pt. Reyes National Shore Park, California. Red and yellow colors indicate the internal distribution of two different oxidation states of sulfur (S(IV) and S(VI)) inside individual particles[111]. (Panel F) Atmospheric dust particles collected at ground site on Okinawa Island, Japan. Color scale indicates fraction of Fe(II) present in individual particles[112]. (Panel G) Marine particles (blue) internally mixed with anthropogenic organic material (green) collected aboard G-1 aircraft during research flight in the vicinity of Sacramento, California[113].

The additional measurements at the ENA site will be examined together with routine data sets. Collectively, they provide continuous characterizations of trace gases (CO and ozone), size spectrum of ambient aerosol and that processed by a thermal denuder, aerosol composition, mixing state, hygroscopicity, CCN spectrum, and optical properties. These long-term measurements will provide seasonal context for the G-1 deployments during the two IOPs, and will be analyzed statistically together with back-trajectory analysis to understand the seasonal variation of climatically relevant properties of aerosol, and its sources and sinks. For example, particle hygroscopicity will be derived from size-resolved CCN spectrum and HTDMA measurements, and its seasonal variation will be examined with the seasonal variation of biological activities (i.e., as indicted by satellite-derived Chl-*a* map). This will provide important insights into the enrichment of organics in SSA due to biological activities, as well as its impact on particle hygroscopicity, mixing state, and CCN population.

2.1.2 Removal of MBL CCN by Droplet Coalescence Scavenging

The simultaneous characterizations of aerosol, cloud, and drizzle fields allow us to systematically examine the removal of the aerosol by coalescence scavenging. Detailed vertical structure and mesoscale variations in both aerosol and cloud fields can provide insights into the aerosol removal and transport, as well as aerosol sources. For example, we will examine if the ultra-clean aerosol layers as observed during VOCALS-REx also exist in the Azores. The measured cloud microphysics and drizzle fields will be used to estimate the rate of CCN removal by coalescence scavenging. The removal rate and its impact on the MBL CCN budget will be examined for clouds with different mesoscale structures and precipitation characteristics. The CCN budget and its controlling processes will also be examined using model simulations constrained by observations. The validated simulations will allow us to quantify processes that cannot be easily obtained by the measurements alone. The details are described in the modelling section (2.5).

2.2 Effects of Aerosol on Clouds and Precipitation (Dong, Jefferson, Kollias, Y. Liu, McComiskey, Wang, Wood)

Understanding the effects of aerosol on warm low clouds is one of the key guiding questions for the Cloud-Aerosol-Precipitation Interactions (CAPI) Working Group of DOE Atmospheric System Research (ASR) program. The overall effects can be grouped into two categories: i) the microphysical impact of aerosol particles in the planetary boundary layer on cloud droplet concentration N_d; ii) the impacts of aerosols on the precipitation efficiency of warm rain. Both are poorly quantified in their contribution to the overall aerosol indirect radiative forcing.

2.2.1 The Representativeness of Surface Measurements for CCN at Cloud Base

The long-term ENA measurements can be used to build up statistical relationships between aerosol and CCN properties measured at the surface with cloud microphysical and precipitation characteristics in the clouds above[51,52,114]. However, as the MBL at the ENA site are often decoupled[59] (see details in section 1.1), it is important to understand the extent to which aerosol particles ingested into clouds are well-represented by measurements at the surface. Because the key MBL aerosol sources are the ocean surface and entrainment from the free troposphere[26], the cloud layer may not experience the same aerosol

conditions as the near-surface air in decoupled MBLs. Many aerosol-cloud correlative studies rely on the assumption that surface-measured CCN and aerosol properties are similar to those near the cloud base. Few studies have tested this assumption. With the in situ measurements of the vertical profiles of aerosol and CCN properties from the surface to cloud base, we will focus on validation and improvement of the ARM CCN profile value-added product (VAP), CCNPROF[115,116], and determine how CCN concentrations change from the surface to cloud base under a range of MBL coupling states.

2.2.2 Impact of Aerosol on Cloud Microphysics and Precipitation

The G-1 measurements of aerosols below cloud base and the cloud microphysical properties in clouds will allow us to quantify aerosol effects on cloud microphysical and precipitation properties. The impact of aerosol on cloud microphysics and drizzle will be examined for a broader range of meteorological and cloud conditions, and for different seasons. One of the hypotheses to be tested is whether mean N_d in low clouds during winter is significantly lower than during summer as suggested by satellite- and surface-based retrievals[20] and whether this affects the seasonal cycle of precipitation from low clouds. Further, we will combine the aircraft measurements and precipitation data retrieved from surface-based remote sensing to understand whether higher precipitation rates during winter are controlling the seasonal cycle of N_d or the stronger aerosol source during summer is the main driver of the seasonality.

Determining how the nature and strength of the aerosol impacts on clouds and precipitation vary with different meteorological and cloud conditions is important for understanding the overall aerosol effect. Kim et al.[118] reported a stronger covariance between aerosol loading and cloud droplet number concentration (stronger first indirect effect) in stable and adiabatic clouds. This finding supports the dependence of cloud-aerosol interactions and their strength on cloud regime[119]. In addition, dependence of N_d on aerosol properties and updraft velocity is non-monotonic, and there is a strong need to improve understanding of the regime classification into aerosol-limited and updraft-limited regimes. We plan to investigate the dependency of the first indirect effect on aerosol concentration and meteorological parameters, including inversion strength, updraft velocity, and cloud regime. In addition, a few studies have shown that the effect of aerosols on spectral shape of cloud droplet size distribution (dispersion effect) also exhibits regime dependence, offsetting the Twomey effect in aerosol-limited regime while enhancing the Twomey effect in updraft-limited regime[120-123]. The regime dependence of the dispersion effect will be examined.

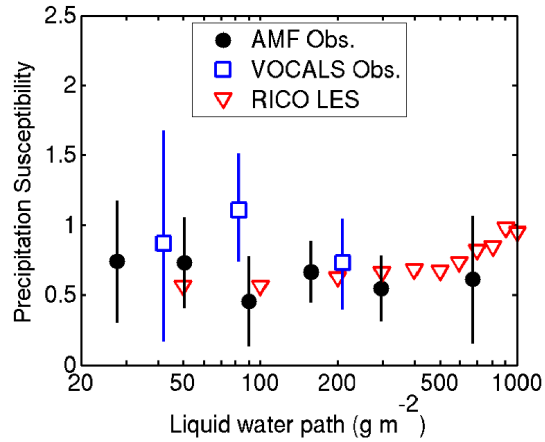

Figure 12. Precipitation intensity susceptibility with respect to CCN number concentration as a function of liquid water path in AMF observations during CAP-MBL and the Convective and Orographically Induced Precipitation Study (COPS) and to cloud droplet number concentration in VOCALS observations averaged over a 5 km length scale (squares) (Figure 7 in Terai et al.[51]), and large-eddy simulations (LES, triangles; adapted from Sorooshian et al.[49]) of precipitating cumulus initialized using soundings from the Rain in Cumulus over the Ocean (RICO) field campaign[117]. Error bars in AMF data represent 95% confidence intervals.

To quantify the relationship between CCN concentration, N_d, and precipitation, we plan to use the precipitation susceptibility metric framework adopted in recent studies (see section 1.1). Considerable differences exist between different approaches for quantifying this metric, even in similar cloud regimes. Susceptibility estimates can be made using aircraft alone[50], with satellite data[49], and with sub-cloud-based remote sensing and in situ-measured aerosol[51,52]. The G-1 aircraft campaign coupled with the surface-based ENA measurements provides arguably the first systematic opportunity to reconcile the different approaches by comparing them for the same cloud systems. We will also examine precipitation susceptibility for clouds with different mesoscale structures (e.g., overcast stratocumulus and open cells) to understand the extent to which different mesoscale regimes have different susceptibilities. Previous measurements suggest that the susceptibility of precipitation *frequency* is reduced in high-LWP clouds[51], but that the susceptibility of precipitation *intensity* is less LWP dependent (Figure 12). However, there is not universal agreement about these dependencies and we will focus upon understanding how susceptibility of both frequency and intensity depends upon cloud liquid water path and thickness. The closely coordinated aircraft- and surface-based measurements also provide improved opportunity to evaluate commonly used autoconversion schemes[73,74,124], to constrain model estimates of accretion, and to understand if models are producing warm rain with the correct balance of accretion and autoconversion[72].

2.3 Cloud Microphysical and Macrophysical Structures, and Entrainment Mixing (Giangrande, Jensen, Kollias, Y. Liu, Miller, Shaw, Wang, Wood)

2.3.1 Cloud Microphysical and Macrophysical Structures

The G-1 payload and the flight plans will provide detailed characterization of the mesoscale variations of cloud and drizzle microphysics, and the co-variance of these fields. The 3D structure provided by the

scanning radars will put the G-1 measurements into mesoscale and cloud lifecycle contexts, allowing better understanding of the processes controlling the observed mesoscale variations and co-variance. The simultaneous measurements of aerosol properties will also provide insights into the impact of the aerosol on the mesoscale variations of the cloud and drizzle field. The mesoscale variations will be examined under representative boundary-layer conditions and cloud regimes. Some of the hypotheses that will be tested include 1) The strong correlation between cloud droplet concentration and liquid water content (LWC) across closed mesoscale cells is a combination of a) CCN loss by coalescence and precipitation and b) the coincidence of stronger updrafts and lower cloud base in the center of the cells. 2) Active-versus-quiescent cells in open-cell conditions represent different times in the cloud lifecycle rather than being distinct types. 3) Drizzle mesoscale organization and precipitation rate are strongly coupled to mesoscale variability of liquid water content and vertical velocity.

We will use the in situ measurements, combined with retrievals from remote sensing at the ENA site, to examine the cold pool and its relationship to mesoscale organizations of cloud and drizzle. While cold pools are generally associated with deep convective systems in which cooling through evaporation or melting of precipitation drives downward motion that spreads out at the surface and influences subsequent growth and organization[125-129], cold pools are also observed in shallow, lightly precipitating cloud conditions[26,130-134] and several studies have suggested that they play an important role in the mesoscale organization of boundary-layer clouds[12,135,136]. Using aircraft observations during the VOCALS-REx campaign, Terai and Wood[133] found that cold pools generally form under heavy drizzle conditions (> 1 mm day^{-1}) with typical horizontal length scales on the order of 2-16 km with clustering, generally associated with open cellular cloud conditions, sometimes resulting in much larger cold pools. We hypothesize negative correlations between temperature and specific humidity in the sub-cloud layer of the marine boundary layer, and that they are primarily caused by cold pool formation. We will use a combination of sub-cloud aircraft observations of the thermodynamic and drizzle characteristics, with scanning radar observations of the mesoscale organizations of cloud and drizzle, to quantify the thermodynamic and spatial characteristics of MBL cold pools and how those characteristics relate to drizzle occurrence/properties and cloud/drizzle mesoscale organization.

2.3.2 Entrainment Mixing

The cloud microphysical response to entrainment and turbulent mixing at cloud top and sides will be another focus of this research theme. Specifically, two questions will be investigated: First, how does the entrainment rate in stratocumulus clouds depend on cloud-top wind shear? Katzwinkel et al.[137] showed fine-scale measurements of the thermodynamic and turbulent properties of the cloud-top entrainment interfacial layer, and suggested that the layer adjusts to a thickness such that shear production is balanced by buoyant suppression. Measurements at cloud top will be used to further investigate the response to both locally-induced, and large-scale-imposed shear. We will examine the entrainment rate[138,139], and explore the relationships between entrainment rate, thermodynamic stability and wind shear above cloud top, and coupling structure below cloud base.

Second, what is the prevalent entrainment mixing mechanism, and what are the controlling factors? There is evidence, for example, that the nature of the microphysical response may be related to cloud life cycle and to aerosol properties[140]. Whether mixing leads to uniform evaporation of all droplets (homogeneous) or total evaporation of a subset of droplets (inhomogeneous) will determine microphysical properties at cloud top, a region especially important for drizzle formation and cloud radiative properties. We will take

advantage of the unique capability of HOLODEC, which provides holograms representing approximately 20 cubic centimeters of cloud air. Under typical stratocumulus conditions each sampled region of cloud will result in a statistically robust estimate of the cloud droplet size distribution, without the loss of information inherent in averaging over long distances. The resulting "local" cloud droplet size distribution is of interest because these are the droplets that interact on microphysical scales. This will give a unique view of entrainment, especially into the process of inhomogeneous versus homogeneous mixing, where the shape of the size distribution within individual mixing events is of relevance[141]. We will also examine the relationship between the recently proposed microphysical measure (homogeneous mixing degree) and dynamical measure (transition scale number) for possible parameterizations of mixing mechanisms[85,90,142].

2.4 Advancing Retrievals of Turbulence, Cloud, and Drizzle (Chiu, Dong, Kollias, Luke)

In the last two decades, several algorithms have been developed that combine radar observations with other data sources to derive the microphysical properties of low-level stratiform clouds. These algorithms are based on synergistic measurements from radars, lidars, and shortwave spectrometers[92,94,96,98,143,144]. The payload of the G-1 provides redundant measurements of turbulence, liquid water content, and size spectrum of cloud droplets and drizzle drops surrounding the ENA site, which will be extremely valuable for evaluating both assumptions introduced in the following retrievals and their performance (e.g., uncertainties and biases).

2.4.1 Validating Retrievals from Vertically Pointing Observations

2.4.1.1 Vertical Air Motion and Eddy Dissipation Rate

A novel technique has been developed to decompose the microphysical and dynamical contributions in the mean Doppler velocity and radar Doppler spectrum width[99]. This technique allows seamless dynamical retrievals of vertical air motion and eddy dissipation rates below and above the cloud base, independent of the presence or not of drizzle particles. The decomposition is based on the assumption that vertical air motion and particle sedimentation velocity are uncorrelated (for example, there is no systematic downdraft during drizzling periods above the cloud base). Furthermore, the eddy dissipation rate technique is based on the assumption that the fast Fourier transform (FFT) of the radar mean Doppler velocity time series can be used to extract the eddy dissipation rate for both drizzling and non-drizzling conditions. These two assumptions will be evaluated using the G-1 vertical air motion measurements during straight legs within the cloud layer in the vicinity of the ENA site. The retrieved vertical air motion and eddy dissipation rates will be compared to those derived from in situ measurements.

2.4.1.2 Drizzle

Drizzle retrievals require assumption of the shape (lognormal or gamma) of the drizzle drop size distribution. This applies to radar-only, radar-lidar, and radar Doppler spectra techniques. The selection of the distribution shape can have a large impact on the retrieved drizzle flux[94]. In addition to the shape of the drizzle distribution, we will also evaluate another assumption employed in the ENCORE method proposed by Fielding et al.[98], and examine whether the normalized drizzle drop number concentration within cloud increases with height with the same gradient as at cloud base. The G-1 observations during

the short legs and spirals around the ENA site will provide comprehensive drizzle measurements below and above the cloud base, which will be used to determine the most appropriate analytical form for representing the drizzle drop size distribution, and to evaluate the assumptions employed in the retrievals under a wide range of cloud conditions.

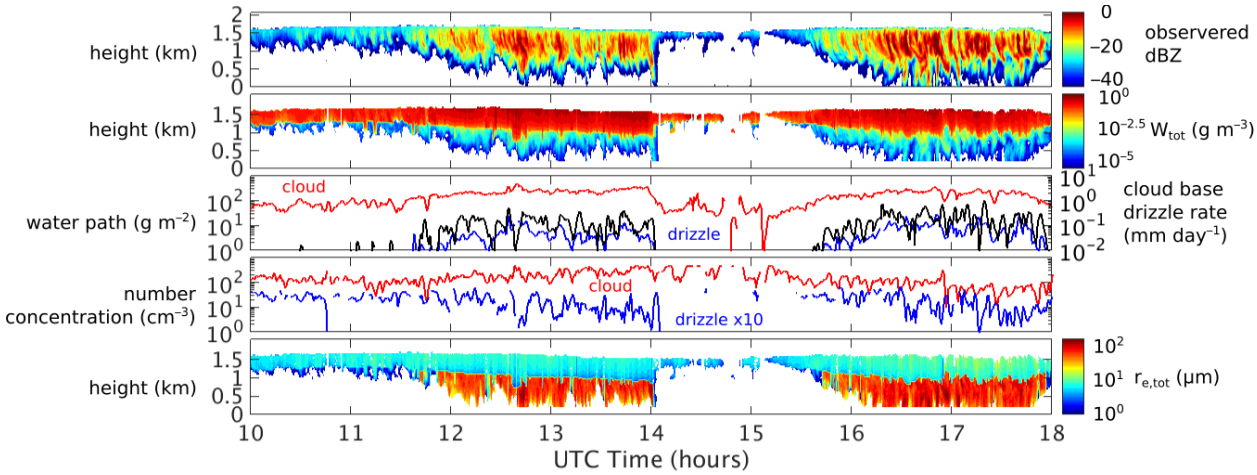

Figure 13. Retrieved cloud properties in predominantly drizzling conditions on 17 September 2009 at the Azores from the ENCORE method98. Panels from top to bottom show time series of observed radar reflectivity factor, retrieved total water content, retrieved cloud (red) and drizzle (blue) liquid water path and cloud base drizzle rate (black), retrieved cloud droplet number concentration (red) and drizzle droplet number concentration multiplied by 10 (blue), and retrieved total effective radius.

2.4.1.3 Clouds

Under non-precipitating conditions, the retrieval of cloud LWC is based on radar-radiometer technique[143]. The inclusion of shortwave measurements enables retrievals of cloud effective radius[98,144]. The in situ microphysical measurements during non-precipitating conditions will allow us to evaluate the assumptions involved (e.g., cloud distribution shape). Under drizzling conditions, the retrieval of the LWC profile is more challenging due to the impact of the drizzle particles on the observed radar reflectivity. We will use the G-1 measurements of cloud LWC profile near the ENA site during drizzling conditions to evaluate cloud/drizzle retrievals (see examples in Figure 13) and to investigate if a linearly increasing LWC profile scaled by the LWP a good assumption for stratiform clouds with and without drizzle.

2.4.1.4 Cumulus Dynamics and Microphysical Retrievals

Compared to stratiform clouds, there has been less research on cloud and drizzle retrievals for shallow cumulus clouds due to their broken nature. For non-precipitating cumulus, Fielding et al.[98,103] have demonstrated the capability of capturing these relatively inhomogeneous clouds with low liquid water path. Additionally, the radar Doppler moments can be used to retrieve the vertical air motion and eddy dissipation rate (e.g., Kollias et al.[145]). However, such retrieval is challenging in the presence of rain. The available multi-wavelength radar observations (K-band, W-band and ultra-high frequency [UHF]) and lidars (ceilometer and Doppler lidars) offer opportunities for retrievals using scattering and absorption at different scattering regimes. However, an extensive microphysical and dynamical dataset is needed to

develop and evaluate these algorithms. We plan to use the shallow cumulus fields characterized by the G-1 at multiple levels above and below the cloud base to support these retrieval evaluation and development activities.

2.4.2 3D Cloud and Drizzle Retrievals from Scanning Radars

In addition to the profiling retrievals for stratocumulus and cumulus, the G-1 observations also provide invaluable data sets for evaluating off-nadir (3D) retrievals of clouds and drizzle properties. In addition to 3D cloud fields from ENCORE (see Sec. 1.1), the SACR2 dual-wavelength observations also enable the retrieval of 3D LWC structure[146,147]. We will use the aircraft observations in distances up to 5 km away from the SACR2 location to evaluate these retrieval techniques that have yet to be tested using in situ observations. In addition to the LWC retrievals, the SACR2 and the XSAPR2 will provide 3D drizzle retrievals at the cloud base height. The scanning radar drizzle-rate retrievals will be based on a Ze-R where the coefficients (prefactor and exponent) will be estimated from the profiling observations. However, the extrapolation of the Ze-R relationship from the column to 3D and ranges up to 40 km requires a good understanding of possible island effects that could alter the drizzle microphysics as a function of distance from the island. The G-1 flight plans include detailed characterizations of turbulence, cloud, and drizzle fields both over the ENA site and upwind over ocean. This will allow us to systematically compare these measured quantities, including their vertical and mesoscale variations over land and ocean for understanding and quantifying the potential uncertainties in retrievals due to island effects. The uncertainty in retrievals will be examined under representative meteorological and cloud conditions (e.g., overcast stratocumulus and open cell structures).

2.5 Model Evaluation and Processes Studies (Bretherton, Fast, Gettelman, Ghan, X. Liu, Y. Liu)

2.5.1 Comparison of Model Simulations with Observations

A key objective of ACE-ENA is intelligent comparison of the data with predictions of both LES and global models in the critical cloud regimes around the ENA site. We will use a suite of modeling tools, including Large Eddy Simulation (LES), mesoscale models such as the Weather Research and Forecasting (WRF) model and global climate models, such as the Community Earth System Model (CESM) and the Accelerated Climate Model for Energy (ACME).

2.5.1.1 Global Modeling

CESM[148] is a comprehensive global earth system model. The atmospheric component (the Community Atmosphere Model, CAM) features a comprehensive two-moment bulk cloud microphysics scheme[149] that is coupled to a two-moment and seven-mode modal aerosol model[150]. The cloud microphysics scheme provides a consistent treatment of cloud precipitation processes, including drizzle formation, prognostic precipitation, and also the interactions between clouds and aerosols in stratiform, and now even convective clouds (with advanced development versions). Advanced versions of CESM also contain a higher-order closure turbulence scheme[151] that represents sub-grid variability for shallow clouds commonly observed at the ENA site. As these same parameterizations are shared with the DOE ACME, our work will be applicable to both models. CESM can be run in several different modes for comparison

to observations. For the G-1 measurements, we will carry out statistical comparisons along flight tracks, using 'specified' or 'nudged' meteorology to constrain synoptic weather systems. CESM can also be run in forecast mode over the region and time period of the campaign. Such techniques have shown promise to reproduce cloud microphysics for synoptic systems, and we will use these methods statistically in shallow cumulus cloud environments. We will also develop a forcing data set to drive CESM in single-column mode for the ENA site, and CESM output files for each of the aircraft flight tracks over the duration of the deployments. This framework will be made available to the community so others can also easily run simulations to compare to the observations.

2.5.1.2 Large-Eddy Simulations

Besides GCMs, local simulations with LES models will be carried out using boundary conditions from the GCM ‘specified’ or ‘nudged’ meteorology runs and/or measured aerosol, cloud and thermodynamic profiles for initialization, together with reanalysis to specify horizontal advective tendencies and vertical motion profiles. One of such models to be employed is the chemistry version of WRF, WRF-Chem, which simulates trace gases and aerosols simultaneously with the meteorological fields[152]. It also includes full online interactions between aerosols, radiation, and clouds for the direct, semi-direct, and first and second indirect effects[153-156]. WRF-Chem simulations will use a LES configuration with horizontal grid spacing of 10-100 m and a domain encompassing a portion of the aircraft sampling over the ocean. The purpose of these simulations is to represent the detailed cloud and aerosol processes over a period of several hours that can be directly compared with the high-temporal (1 Hz) aircraft measurements. In addition, the LES simulations will also be used to synthesize numerous measurement types onboard the G-1 and at the ENA site.

The comparisons with observations allow us to evaluate, constrain, and improve model parameterizations. Many of the developers of the CESM/ACME parameterizations critical for cloud microphysics (Gettelman) and aerosols (Liu, Ghan) are part of the ACE-ENA team, and will use the analyses and sensitivity tests below to improve future versions of CESM/ACME. Comparisons between the global model, LES, and observations will be performed for critical cloud regimes. Key comparisons will include aerosol size spectrum, chemical composition, cloud, and drizzle properties. For LES simulations, comparisons will also focus on the horizontal variation and vertical structure of aerosol, cloud, precipitation, and co-variance of these fields, such as the strong correlation between droplet concentration and LWC across closed mesoscale cells. Besides the comparison of CESM simulations using 'specified' or 'nudged' meteorology with aircraft observations, climatologies from free-running simulations and simulations using a single-column version of CESM will also be compared to those observed at the ENA site and to LES simulations.

In addition to the standard global model configuration, several sets of sensitivity tests will be carried out. These sensitivity tests will include model physics related to aerosol treatment in the GCM (e.g., emissions, aging, wet scavenging) and simulations at higher horizontal resolutions (e.g. 1, 0.5 and 0.25 degrees) that resolve the mesoscale dynamics, which are important for the aerosol transport from continents to the ENA site. The comparisons will also include the relationships among aerosol, cloud, and precipitation properties. For example, simulated relationship between droplet number and CCN concentration and the relationship between cloud optical depth and droplet number, both of which drive the aerosol effects on cloud radiative forcing, will be constrained using observations. We will also compare simulated and observed estimates of the sensitivity of the precipitation probability to the aerosol

(S_{pop})[52,70]. Through these comparisons, potential biases in the aerosol and cloud simulations in CESM and LES will be identified, and improvements can be made under representative synoptic conditions and aerosol regimes.

2.5.2 Understanding the Controlling Processes for Aerosol Budget, Cloud Lifecycle, and Aerosol Cloud Interactions Using Validated/Constrained Model Simulations

The systematic comparisons between the simulated and observed aerosol, cloud, and precipitation fields will allow the development and validation of more realistic simulations that replicate the aircraft measurements. The validated simulations and models can then be used to quantify processes that cannot be obtained directly from the aircraft measurements. We will use the validated LES and GCM simulations to examine the budgets of mass mixing ratio of different aerosol types and aerosol number concentrations in the MBL and in the free troposphere over the region covering the ENA site. These budget analyses will be conducted at different time scales (daily versus monthly), at different spatial scales (mesoscales versus GCM grid scales), and in different seasons (summer versus winter).

We will use an aerosol-coupled LES model (e.g., WRF-Chem) to examine the processes driving the vertical and mesoscale structures of aerosol, cloud, and drizzle, and co-variance of these fields. This will enable us to obtain new process-level understanding of aerosol budget, cloud lifecycle, and aerosol cloud interactions, and form the basis of developing and testing new parameterizations suitable for spatial scales used by the next generation of climate models. For example, we will examine if the strong correlation between droplet concentration and LWC across closed mesoscale cells is solely related to the coincidence of stronger updrafts and lower cloud base in the center of the cells, or if drizzle and entrainment are also contributing factors. We will also perform LES case studies for different regimes (e.g., low versus high aerosol, different aerosol sources, different aerosol layering) observed during the campaign to investigate how the differences in aerosol sources and meteorology affect the cloud lifecycle. Both simulation categories will be evaluated using aerosol and cloud properties obtained from the aircraft measurements as well as the continuous observations at the ENA site.

3.0 Relevancy

The ACE-ENA deployments squarely fit the mission and vision of DOE Office of Biological and Environmental Research, Climate and Environmental Sciences Division. Presently, low clouds are poorly represented in global climate models, and the response of low clouds to changes in atmospheric greenhouse gases and aerosols remains the major source of uncertainty in climate simulations. The deployments will provide detailed characterizations of boundary-layer and lower FT structure, and associated vertical distributions and horizontal variations of low clouds and aerosol in the Azores under representative meteorological and cloud conditions. This information is critical for understanding and improving the representation of the MBL aerosol budget, the lifecycle of marine low clouds, and the MBL's response to aerosol perturbations. Data from the deployments will be used to improve representations of low clouds in climate and earth system models, therefore reducing the uncertainties in climate and earth system models toward the development of sustainable solutions for the nation's energy and environmental challenges.

4.0 References

1 Bony, S. & Dufresne, J. L. Marine boundary layer clouds at the heart of tropical cloud feedback uncertainties in climate models. *Geophys. Res. Lett.* **32**, doi:10.1029/2005gl023851 (2005).

2 Lohmann, U. & Feichter, J. Global indirect aerosol effects: a review. *Atmos. Chem. Phys.* **5**, 715-737 (2005).

3 Wyant, M. C. *et al.* A comparison of low-latitude cloud properties and their response to climate change in three AGCMs sorted into regimes using mid-tropospheric vertical velocity. *Climate Dynamics* **27**, 261-279, doi:10.1007/s00382-006-0138-4 (2006).

4 Bony, S. *et al.* How well do we understand and evaluate climate change feedback processes? *J. Climate* **19**, 3445–3482 (2006).

5 Allan, R. P., Slingo, A., Milton, S. F. & Brooks, M. A. Evaluation of the Met Office global forecast model using Geostationary Earth Radiation Budget (GERB) data. *Q. J. Roy. Meteorol. Soc.* **133**, 1993–2010 (2007).

6 Nam, C., Bony, S., Dufresne, J. L. & Chepfer, H. The 'too few, too bright' tropical low-cloud problem in CMIP5 models. *Geophys. Res. Lett.* **39**, n/a-n/a, doi:10.1029/2012GL053421 (2012).

7 Webb, M. J., Lambert, F. H. & Gregory, J. M. Origins of differences in climate sensitivity, forcing and feedback in climate models. *Clim. Dyn.* **40**, 677–707 (2013).

8 Stephens, G. L. Is there a missing low cloud feedback in current climate models? *GEWEX News* **20**, 5–7 (2010).

9 Suzuki, K., Nakajima, T., Nakajima, T. Y. & Khain, A. P. A Study of Microphysical Mechanisms for Correlation Patterns between Droplet Radius and Optical Thickness of Warm Clouds with a Spectral Bin Microphysics Cloud Model. *J. Atmos. Sci.* **67**, 1126-1141, doi:10.1175/2009JAS3283.1 (2009).

10 Albrecht, B. A. Aerosols, cloud microphysics, and fractional cloudiness. *Science* **245**, 1227-1230 (1989).

11 Pincus, R. & Baker, M. B. Effect of precipitation on the albedo susceptibility of clouds in the marine boundary-layer. *Nature* **372**, 250-252, doi:10.1038/372250a0 (1994).

12 Feingold, G., Koren, I., Wang, H. L., Xue, H. W. & Brewer, W. A. Precipitation-generated oscillations in open cellular cloud fields. *Nature* **466**, 849-852, doi:10.1038/nature09314 (2010).

13 Twomey, S. Influence of pollution on shortwave albedo of clouds. *J. Atmos. Sci.* **34**, 1149-1152 (1977).

14 Carslaw, K. S. *et al.* Large contribution of natural aerosols to uncertainty in indirect forcing. *Nature* **503**, 67-71, doi:10.1038/nature12674 (2013).

15 Kooperman, G. J., Pritchard, M. S. & Somerville, R. C. J. Robustness and sensitivities of central US summer convection in the super-parameterized CAM: Multi-model intercomparison with a new regional EOF index. *Geophys. Res. Lett.* **40**, 3287-3291, doi:10.1002/grl.50597 (2013).

16 Isaksen, I. S. A. *et al.* Atmospheric composition change: Climate-Chemistry interactions. *Atmos. Environ.* **43**, 5138-5192, doi:10.1016/j.atmosenv.2009.08.003 (2009).

17 IPCC. *Climate Change 2013: The Physical Science Basis: Contribution of Working Group I to the Fourth Assessment Report of the Intergovernmental Panel on Climate Change*. (Cambridge University Press, 2013).

18 Rosenfeld, D., Sherwood, S., Wood, R. & Donner, L. Climate Effects of Aerosol-Cloud Interactions. *Science* **343**, 379-380 (2014).

19 Rosenfeld, D. *et al.* Global observations of aerosol-cloud-precipitation-climate interactions. *Rev. Geophys.* **52**, 750-808, doi:10.1002/2013RG000441 (2014).

20 Wood, R. *et al.* Clouds, Aerosol, and Precipitation in the Marine Boundary Layer: An ARM Mobile Facility Deployment. *Bull. Am. Meteorol. Soc.* **In press** (2015).

21 Hamilton, D. S. *et al.* Occurrence of pristine aerosol environments on a polluted planet. *Proc. Natl. Acad. Sci. USA* **111**, 18466-18471, doi:10.1073/pnas.1415440111 (2014).

22 Tselioudis, G., Rossow, W., Zhang, Y. C. & Konsta, D. Global Weather States and Their Properties from Passive and Active Satellite Cloud Retrievals. *J. Climate* **26**, 7734-7746, doi:10.1175/jcli-d-13-00024.1 (2013).

23 Quinn, P. K. & Bates, T. S. The case against climate regulation via oceanic phytoplankton sulphur emissions. *Nature* **480**, 51-56, doi:10.1038/nature10580 (2011).

24 Clarke, A. D. *et al.* Particle production in the remote marine atmosphere: Cloud outflow and subsidence during ACE 1. *J. Geophys. Res.* **103**, 16397-16409, doi:10.1029/97jd02987 (1998).

25 Hudson, J. G. & Xie, Y. H. Vertical distributions of cloud condensation nuclei spectra over the summertime northeast Pacific and Atlantic Oceans. *J. Geophys. Res.* **104**, 30219-30229, doi:10.1029/1999jd900413 (1999).

26 Wood, R., Leon, D., Lebsock, M., Snider, J. & Clarke, A. D. Precipitation driving of droplet concentration variability in marine low clouds. *J. Geophys. Res.* **117**, doi:10.1029/2012jd018305 (2012).

27 Russell, L. M. *et al.* Bidirectional mixing in an ACE 1 marine boundary layer overlain by a second turbulent layer. *J. Geophys. Res.* **103**, 16411-16432, doi:10.1029/97jd03437 (1998).

28 Frossard, A. A. *et al.* Sources and composition of submicron organic mass in marine aerosol particles. *J. Geophys. Res.* **119**, 12977-13003, doi:10.1002/2014jd021913 (2014).

29 Petters, M. D. *et al.* Accumulation mode aerosol, pockets of open cells, and particle nucleation in the remote subtropical Pacific marine boundary layer. *J. Geophys. Res.* **111**, doi:10.1029/2004jd005694 (2006).

30 Tomlinson, J. M., Li, R. J. & Collins, D. R. Physical and chemical properties of the aerosol within the southeastern Pacific marine boundary layer. *J. Geophys. Res.* **112**, doi:10.1029/2006jd007771 (2007).

31 Wood, R. *et al.* An aircraft case study of the spatial transition from closed to open mesoscale cellular convection over the Southeast Pacific. *Atmos. Chem. Phys.* **11**, 2341-2370, doi:10.5194/acp-11-2341-2011 (2011).

32 Kazil, J. *et al.* Modeling chemical and aerosol processes in the transition from closed to open cells during VOCALS-REx. *Atmos. Chem. Phys.* **11**, 7491-7514, doi:10.5194/acp-11-7491-2011 (2011).

33 Val Martin, M., Honrath, R. E., Owen, R. C. & Li, Q. B. Seasonal variation of nitrogen oxides in the central North Atlantic lower free troposphere. *J. Geophys. Res.* **113**, D17307, doi:doi:10.1029/2007JD009688. (2008).

34 Clarke, A. D. *et al.* Free troposphere as a major source of CCN for the equatorial pacific boundary layer: long-range transport and teleconnections. *Atmos. Chem. Phys.* **13**, 7511-7529, doi:10.5194/acp-13-7511-2013 (2013).

35 Stemmler, J. D., Wood, R. & Bretherton, C. S. Low CCN concentration events at a remote site in the eastern Atlantic: seasonality, meteorology and causes *J. Geophys. Res.* **In preparation** (2015).

36 O'Dowd, C. D. *et al.* Biogenically driven organic contribution to marine aerosol. *Nature* **431**, 676-680 (2004).

37 Quinn, P. K. *et al.* Contribution of sea surface carbon pool to organic matter enrichment in sea spray aerosol. *Nature Geoscience* **7**, 228-232, doi:10.1038/ngeo2092 (2014).

38 McCoy, D. T. *et al.* Natural aerosols explain seasonal and spatial patterns of Southern Ocean cloud albedo. *Science Advances* **In revision** (2015).

39 Rinaldi, M. *et al.* Is chlorophyll-a the best surrogate for organic matter enrichment in submicron primary marine aerosol? *J. Geophys. Res.* **118**, 4964-4973, doi:10.1002/jgrd.50417 (2013).

40 Burrows, S. M. *et al.* A physically based framework for modeling the organic fractionation of sea spray aerosol from bubble film Langmuir equilibria. *Atmos. Chem. Phys.* **14**, 13601-13629, doi:10.5194/acp-14-13601-2014 (2014).

41 Baker, M. B. & Charlson, R. J. Bistability of CCN concentrations and thermodynamics in the could-topped boundary-layer. *Nature* **345**, 142-145, doi:10.1038/345142a0 (1990).

42 Feingold, G., Kreidenweis, S. M., Stevens, B. & Cotton, W. R. Numerical simulations of stratocumulus processing of cloud condensation nuclei through collision-coalescence. *J. Geophys. Res.* **101**, 21391-21402, doi:10.1029/96jd01552 (1996).

43 Wood, R. Rate of loss of cloud droplets by coalescence in warm clouds. *J. Geophys. Res.* **111**, doi:10.1029/2006jd007553 (2006).

44 Stemmler, I., Hense, I. & Quack, B. Marine sources of bromoform in the global open ocean - global patterns and emissions. *Biogeosciences* **12**, 1967-1981, doi:10.5194/bg-12-1967-2015 (2015).

45 Terai, C. R., Bretherton, C. S., Wood, R. & Painter, G. Aircraft observations of aerosol, cloud, precipitation, and boundary layer properties in pockets of open cells over the southeast Pacific. *Atmos. Chem. Phys.* **14**, 8071-8088, doi:10.5194/acp-14-8071-2014 (2014).

46 Feingold, G., Eberhard, W. L., Veron, D. E. & Previdi, M. First measurements of the Twomey indirect effect using ground-based remote sensors. *Geophys. Res. Lett.* **30**, doi:10.1029/2002gl016633 (2003).

47 Painemal, D. & Zuidema, P. The first aerosol indirect effect quantified through airborne remote sensing during VOCALS-REx. *Atmos. Chem. Phys.* **13**, 917-931, doi:10.5194/acp-13-917-2013 (2013).

48 Feingold, G. & Siebert, H. Cloud-Aerosol Interactions from the Micro to the Cloud Scale. *Clouds in the Perturbed Climate System: Their Relationship to Energy Balance, Atmospheric Dynamics, and Precipitation*, 319-338 (2009).

49 Sorooshian, A., Feingold, G., Lebsock, M. D., Jiang, H. L. & Stephens, G. L. On the precipitation susceptibility of clouds to aerosol perturbations. *Geophys. Res. Lett.* **36**, doi:10.1029/2009gl038993 (2009).

50 Sorooshian, A., Feingold, G., Lebsock, M. D., Jiang, H. L. & Stephens, G. L. Deconstructing the precipitation susceptibility construct: Improving methodology for aerosol-cloud precipitation studies. *J. Geophys. Res.* **115**, doi:10.1029/2009jd013426 (2010).

51 Terai, C. R., Wood, R., Leon, D. C. & Zuidema, P. Does precipitation susceptibility vary with increasing cloud thickness in marine stratocumulus? *Atmos. Chem. Phys.* **12**, 4567-4583, doi:10.5194/acp-12-4567-2012 (2012).

52 Mann, J. A. L. *et al.* Aerosol impacts on drizzle properties in warm clouds from ARM Mobile Facility maritime and continental deployments. *J. Geophys. Res.* **119**, 4136-4148, doi:10.1002/2013jd021339 (2014).

53 Ackerman, A. S., Kirkpatrick, M. P., Stevens, D. E. & Toon, O. B. The impact of humidity above stratiform clouds on indirect aerosol climate forcing. *Nature* **432**, 1014-1017, doi:10.1038/nature03174 (2004).

54 Wood, R. Cancellation of aerosol indirect effects in marine stratocumulus through cloud thinning. *J. Atmos. Sci.* **64**, 2657-2669, doi:10.1175/jas3942.1 (2007).

55 Chen, Y. C. *et al.* Occurrence of lower cloud albedo in ship tracks. *Atmos. Chem. Phys.* **12**, 8223-8235, doi:10.5194/acp-12-8223-2012 (2012).

56 Coakley, J. A. & Walsh, C. D. Limits to the aerosol indirect radiative effect derived from observations of ship tracks. *J. Atmos. Sci.* **59**, 668-680, doi:10.1175/1520-0469(2002)059<0668:lttair>2.0.co;2 (2002).

57 Chen, Y. C. *et al.* A comprehensive numerical study of aerosol-cloud-precipitation interactions in marine stratocumulus. *Atmos. Chem. Phys.* **11**, 9749-9769, doi:10.5194/acp-11-9749-2011 (2011).

58 Christensen, M. W. & Stephens, G. L. Microphysical and macrophysical responses of marine stratocumulus polluted by underlying ships: Evidence of cloud deepening. *J. Geophys. Res.* **116**, doi:10.1029/2010jd014638 (2011).

59 Remillard, J., Kollias, P., Luke, E. & Wood, R. Marine Boundary Layer Cloud Observations in the Azores. *J. Climate* **25**, 7381-7398, doi:10.1175/jcli-d-11-00610.1 (2012).

60 Bretherton, C. S., Austin, P. & Siems, S. T. Cloudness and marine boundary-layer dynamics in the ASTEX Lagrangian experiments. Part II: Cloudness, drizzle, surface fluxes, and entrainment. *J. Atmos. Sci.* **52**, 2724-2735, doi:10.1175/1520-0469(1995)052<2724:cambld>2.0.co;2 (1995).

61 Painemal, D., Minnis, P. & Nordeen, M. Aerosol variability, synoptic-scale processes, and their link to the cloud microphysics over the northeast Pacific during MAGIC. *J. Geophys. Res.* **Accepted** (2015).
62 Chan, K. M. & Wood, R. The seasonal cycle of planetary boundary layer depth determined using COSMIC radio occultation data. *J. Geophys. Res.* **118**, 12,422-412,434, doi:doi:10.1002/2013JD020147. (2013).
63 Dong, X. Q., Schwartz, A., Xi, B. K. & Wu, P. Investigation of the Marine Boundary Layer Cloud Properties under the Coupled and Decoupled conditions over the Azores. *J. Geophys. Res.* **Accepted** (2015).
64 Martin, G. M., Johnson, D. W. & Spice, A. The measurement and parameterization of effective radius of rroplets In warm stratocumulus dlouds. *J. Atmos. Sci.* **51**, 1823-1842 (1994).
65 Twomey, S. The nuclei of natural cloud formation, Part I: The chemical diffusion method and its application to atmospheric nuclei. *Geophisica pura e applicata* **43**, 227-242 (1959).
66 Twomey, S. The nuclei of natural cloud formation, Part II: The supersaturation in natural clouds and the variation of cloud droplet concentration. *Geophisica pura e applicata* **43**, 243-249 (1959).
67 Mechem, D. B., Yuter, S. E. & de Szoeke, S. P. Thermodynamic and Aerosol Controls in Southeast Pacific Stratocumulus. *J. Atmos. Sci.* **69**, 1250-1266, doi:10.1175/jas-d-11-0165.1 (2012).
68 Terai, C. R., wood, R. & Kubar, T. L. Satellite and diagnostic model estimates of precipitation susceptibility in low-level, marine stratocumulus. *Submitted to journal of Geophysical Research* (2015).
69 L'Ecuyer, T. S., Berg, W., Haynes, J., Lebsock, M. & Takemura, T. Global observations of aerosol impacts on precipitation occurrence in warm maritime clouds. *J. Geophys. Res.* **114**, doi:10.1029/2008jd011273 (2009).
70 Wang, M. H. *et al.* Constraining cloud lifetime effects of aerosols using A-Train satellite observations. *Geophys. Res. Lett.* **39**, doi:10.1029/2012gl052204 (2012).
71 Wood, R., Kubar, T. L. & Hartmann, D. L. Understanding the importance of microphysics and macrophysics for warm rain in marine low clouds: Part II. Heuristic models of rain formation. *J. Atmos. Sci.* **66**, 2973-2990, doi:doi: 10.1175/2009JAS3072.1 (2009).
72 Gettelman, A., Morrison, H., Terai, C. R. & Wood, R. Microphysical process rates and global aerosol-cloud interactions. *Atmos. Chem. Phys.* **13**, 9855-9867, doi:10.5194/acp-13-9855-2013 (2013).
73 Wood, R. Drizzle in stratiform boundary layer clouds. Part 1: Vertical and horizontal structure. *J. Atmos. Sci.* **62**, 3011-3033, doi:10.1175/jas3529.1 (2005).
74 Wood, R. Drizzle in stratiform boundary layer clouds. Part II: Microphysical aspects. *J. Atmos. Sci.* **62**, 3034-3050, doi:10.1175/jas3530.1 (2005).
75 Comstock, K. K., Bretherton, C. S. & Yuter, S. E. Mesoscale variability and drizzle in Southeast Pacific stratocumulus. *J. Atmos. Sci.* **62**, 3792-3807, doi:10.1175/jas3567.1 (2005).
76 Bretherton, C. S. *et al.* The Epic 2001 Stratocumulus Study. *Bull. Am. Meteorol. Soc.* **85**, 967-977, doi:10.1175/BAMS-85-7-967 (2004).
77 Muhlbauer, A., McCoy, I. L. & Wood, R. Climatology of stratocumulus cloud morphologies: microphysical properties and radiative effects. *Atmos. Chem. Phys.* **14**, 6695-6716, doi:10.5194/acp-14-6695-2014 (2014).
78 Deardorff, J. W. Cloud top entrainment instability. *J. Atmos. Sci.* **37**, 131-147, doi:10.1175/1520-0469(1980)037<0131:ctei>2.0.co;2 (1980).
79 Bretherton, C. S. & Wyant, M. C. Moisture transport, lower-tropospheric stability, and decoupling of cloud-topped boundary layers. *J. Atmos. Sci.* **54**, 148-167, doi:10.1175/1520-0469(1997)054<0148:mtltsa>2.0.co;2 (1997).
80 Nicholls, S. & Leighton, J. An observation study of the structure of stratiform cloud sheets: Part I. Structure. *Q. J. Roy. Meteor. Soc.* **112**, 431-460, doi:10.1002/qj.49711247209 (1986).
81 Gerber, H. Microphysics of marine stratocumulus clouds with two drizzle modes. *J. Atmos. Sci.* **53**, 1649-1662, doi:10.1175/1520-0469(1996)053<1649:momscw>2.0.co;2 (1996).

82 Wang, Q. & Albrecht, B. A. Observations of cloud-top entrainment in marine stratocumulus clouds. *J. Atmos. Sci.* **51**, 1530-1547, doi:10.1175/1520-0469(1994)051<1530:ooctei>2.0.co;2 (1994).
83 Gerber, H., Frick, G., Malinowski, S. P., Brenguier, J. L. & Burnet, F. Holes and entrainment in stratocumulus. *J. Atmos. Sci.* **62**, 443-459, doi:10.1175/jas-3399.1 (2005).
84 de Roode, S. R. & Wang, Q. Do stratocumulus clouds detrain? FIRE I data revisited. *Boundary-Layer Meteorology* **122**, 479-491, doi:10.1007/s10546-006-9113-1 (2007).
85 Lu, C. S., Liu, Y. G. & Niu, S. J. Examination of turbulent entrainment-mixing mechanisms using a combined approach. *J. Geophys. Res.* **116**, doi:10.1029/2011jd015944 (2011).
86 Yum, S. S. *et al.* Cloud microphysical relationships and their implication on entrainment and mixing mechanism for the stratocumulus clouds measured during the VOCALS project. *J. Geophys. Res.* **In press** (2015).
87 Grabowski, W. W. Indirect impact of atmospheric aerosols in idealized simulations of convective-radiative quasi equilibrium. *J. Climate* **19**, 4664-4682, doi:10.1175/jcli3857.1 (2006).
88 Chosson, F., Brenguier, J. L. & Schuller, L. Entrainment-mixing and radiative transfer simulation in boundary layer clouds. *J. Atmos. Sci.* **64**, 2670-2682, doi:10.1175/jas3975.1 (2007).
89 Lehmann, K., Siebert, H. & Shaw, R. A. Homogeneous and Inhomogeneous Mixing in Cumulus Clouds: Dependence on Local Turbulence Structure. *J. Atmos. Sci.* **66**, 3641–3659 (2009).
90 Lu, C. S., Liu, Y. G., Niu, S. J., Krueger, S. & Wagner, T. Exploring parameterization for turbulent entrainment-mixing processes in clouds. *J. Geophys. Res.* **118**, 185-194, doi:10.1029/2012jd018464 (2013).
91 Lu, C. S., Niu, S. J., Liu, Y. G. & Vogelmann, A. M. Empirical relationship between entrainment rate and microphysics in cumulus clouds. *Geophys. Res. Lett.* **40**, 2333-2338, doi:10.1002/grl.50445 (2013).
92 Frisch, A. S., Fairall, C. W. & Snider, J. B. Measurement of stratus cloud and drizzle parameters in ASTEX with a K_α-band Doppler radar and a microwave radiometer. *J. Atmos. Sci.* **52**, 2788-2799, doi:10.1175/1520-0469(1995)052<2788:moscad>2.0.co;2 (1995).
93 Wu, P., Dong, X. Q. & Xi, B. K. MBL drizzle properties and their impact on cloud microphysical property retrievals. *Atmos. Meas. Tech.* **Accepted** (2015).
94 O'Connor, E. J., Hogan, R. J. & Illingworth, A. J. Retrieving stratocumulus drizzle parameters using Doppler radar and lidar. *J. Appl. Meteorol.* **44**, 14-27, doi:10.1175/jam-2181.1 (2005).
95 Westbrook, C. D., Hogan, R. J., O'Connor, E. J. & Illingworth, A. J. Estimating drizzle drop size and precipitation rate using two-colour lidar measurements. *Atmos. Meas. Tech.* **3**, 671-681, doi:10.5194/amt-3-671-2010 (2010).
96 Luke, E. P. & Kollias, P. Separating Cloud and Drizzle Radar Moments during Precipitation Onset Using Doppler Spectra. *J. Atmos. Oceanic Technol.* **30**, 1656-1671, doi:10.1175/jtech-d-11-00195.1 (2013).
97 Chandrasekar, V. & Nguyen, C. in *2015 ARM / ASR Joint User Facility and Principal Investigators Meeting* (Vienna, Virginia, USA, 2015).
98 Fielding, M. D. *et al.* Joint retrievals of cloud and drizzle in marine boundary layer clouds using ground-based radar, lidar and zenith radiances. *Atmos. Meas. Tech. Discuss.* **8**, 1833-1889 (2015).
99 Luke, E. & Kollias, P. Vertical Air Motion and Eddy Dissipation Rate Retrievals in Low Stratiform Clouds, manuscript in preparation. *Manusript in preparation* (2015).
100 Kollias, P., Bharadwaj, N., Widener, K., Jo, I. & Johnson, K. Scanning ARM Cloud Radars. Part I: Operational Sampling Strategies. *J. Atmos. Oceanic Technol.* **31**, 569-582, doi:10.1175/jtech-d-13-00044.1 (2014).
101 Kollias, P. *et al.* Scanning ARM Cloud Radars. Part II: Data Quality Control and Processing. *J. Atmos. Oceanic Technol.* **31**, 583-598, doi:10.1175/jtech-d-13-00045.1 (2014).
102 Lamer, K., Tatarevic, A., Jo, I. & Kollias, P. Evaluation of gridded scanning ARM cloud radar reflectivity observations and vertical doppler velocity retrievals. *Atmos. Meas. Tech.* **7**, 1089-1103, doi:10.5194/amt-7-1089-2014 (2014).

103 Fielding, M. D., Chiu, J. C., Hogan, R. J. & Feingold, G. A novel ensemble method for retrieving properties of warm cloud in 3-D using ground-based scanning radar and zenith radiances. *J. Geophys. Res.* **119**, 10912-10930, doi:10.1002/2014jd021742 (2014).

104 Fugal, J. P. & Shaw, R. A. Cloud particle size distributions measured with an airborne digital in-line holographic instrument. *Atmos. Meas. Tech.* **2**, 259-271, doi:10.5194/amt-2-259-2009 (2009).

105 Laskin, A., Laskin, J. & Nizkorodov, S. A. Mass spectrometric approaches for chemical characterisation of atmospheric aerosols: critical review of the most recent advances. *Environ. Chem.* **9**, 163-189, doi:10.1071/en12052 (2012).

106 Moffet, R. C. *et al.* Spectro-microscopic measurements of carbonaceous aerosol aging in Central California. *Atmos. Chem. Phys.* **13**, 10445-10459, doi:10.5194/acp-13-10445-2013 (2013).

107 Moffet, R. C. *et al.* Microscopic characterization of carbonaceous aerosol particle aging in the outflow from Mexico City. *Atmos. Chem. Phys.* **10**, 961-976, doi:10.5194/acp-10-961-2010 (2010).

108 Wang, B. *et al.* Heterogeneous ice nucleation and water uptake by field-collected atmospheric particles below 273 K. *J. Geophys. Res.* **117**, D00V19, doi:10.1029/2012jd017446 (2012).

109 Zaveri, R. A. *et al.* Nighttime chemical evolution of aerosol and trace gases in a power plant plume: Implications for secondary organic nitrate and organosulfate aerosol formation, NO_3 radical chemistry, and N_2O_5 heterogeneous hydrolysis. *J. Geophys. Res.* **115**, D12304, doi:10.1029/2009jd013250 (2010).

110 Hand, J. L. *et al.* Optical, physical, and chemical properties of tar balls observed during the Yosemite Aerosol Characterization Study. *J. Geophys. Res.* **110**, D21210, doi:10.1029/2004jd005728 (2005).

111 Liu, Y. *et al.* Internal structure, hygroscopic and reactive properties of mixed sodium methanesulfonate-sodium chloride particles. *Phys. Chem. Chem. Phys.* **13**, 11846-11857 (2011).

112 Moffet, R. C. *et al.* Iron speciation and mixing in single aerosol particles from the Asian continental outflow. *J. Geophys. Res.* **117**, D07204, doi:10.1029/2011jd016746 (2012).

113 Laskin, A. *et al.* Tropospheric chemistry of internally mixed sea salt and organic particles: Surprising reactivity of NaCl with weak organic acids. *J. Geophys. Res.* **117**, D15302, doi:10.1029/2012jd017743 (2012).

114 McComiskey, A. *et al.* An assessment of aerosol-cloud interactions in marine stratus clouds based on surface remote sensing. *J. Geophys. Res.* **114**, doi:10.1029/2008jd011006 (2009).

115 Ghan, S. J. & Collins, D. R. Use of in situ data to test a Raman lidar-based cloud condensation nuclei remote sensing method. *J. Atmos. Oceanic Technol.* **21**, 387-394, doi:10.1175/1520-0426(2004)021<0387:uoisdt>2.0.co;2 (2004).

116 Ghan, S. J. *et al.* Use of in situ cloud condensation nuclei, extinction, and aerosol size distribution measurements to test a method for retrieving cloud condensation nuclei profiles from surface measurements. *J. Geophys. Res.* **111**, doi:10.1029/2004jd005752 (2006).

117 Rauber, R. M. *et al.* Rain in Shallow Cumulus Over the Ocean: The RICO Campaign. *Bull. Am. Meteorol. Soc.* **88**, 1912-1928, doi:10.1175/BAMS-88-12-1912 (2007).

118 Kim, Y. J., Kim, B. G., Miller, M., Min, Q. L. & Song, C. K. Enhanced aerosol-cloud relationships in more stable and adiabatic clouds. *Asia-Pacific Journal of Atmospheric Sciences* **48**, 283-293, doi:10.1007/s13143-012-0028-0 (2012).

119 Stevens, B. & Feingold, G. Untangling aerosol effects on clouds and precipitation in a buffered system. *Nature* **461**, 607-613, doi:10.1038/nature08281 (2009).

120 Liu, Y. G. & Daum, P. H. Anthropogenica erosols - Indirect warming effect from dispersion forcing. *Nature* **419**, 580-581, doi:10.1038/419580a (2002).

121 Hudson, J. G., Noble, S. & Jha, V. Cloud droplet spectral width relationship to CCN spectra and vertical velocity. *J. Geophys. Res.* **117**, doi:10.1029/2012jd017546 (2012).

122 Liu, Y. G., Daum, P. H. & Lu, C. S. Comment on "Cloud droplet spectral width relationship to CCN spectra and vertical velocity" by Hudson et al. *J. Geophys. Res.* **119**, 1874-1877, doi:10.1002/2012jd019207 (2014).

123 Liu, Y. G., Chen, J., Lu, C. & Zhang, M. in *2015 ARM / ASR Joint User Facility and Principal Investigators Meeting* (Vienna, Virginia, USA, 2015).

124 Liu, Y. G., Daum, P. H. & McGraw, R. An analytical expression for predicting the critical radius in the autoconversion parameterization. *Geophys. Res. Lett.* **31**, doi:10.1029/2003gl019117 (2004).

125 Knupp, K. R. & Cotton, W. R. Convective cloud downdrafts - An interpretive survey. *Rev. Sace Phys. Geophys.* **23**, 183-215 (1985).

126 Braham, R. R. The water and energy budgets of the thunderstorm and their relation to thunderstorm development. *J. Meteorol.* **9**, 227-242, doi:10.1175/1520-0469(1952)009<0227:twaebo>2.0.co;2 (1952).

127 Riehl, H. & Malkus, J. S. On the heat balance and maintenance of circulation in the trades. *Q. J. Roy. Meteor. Soc.* **83**, 21-29, doi:10.1002/qj.49708335503 (1957).

128 Zipser, E. J. Mesoscale and convective-scale downdrafts as distinct components of squall-line strcture. *Mon. Weather Rev.* **105**, 1568-1589, doi:10.1175/1520-0493(1977)105<1568:macdad>2.0.co;2 (1977).

129 Gamache, J. F. & Houze, R. A. Mesoscale air motions associated with a tropical squall line. *Mon. Weather Rev.* **110**, 118-135, doi:10.1175/1520-0493(1982)110<0118:mamawa>2.0.co;2 (1982).

130 Jensen, J. B., Lee, S. H., Krummel, P. B., Katzfey, J. & Gogoasa, D. Precipitation in marine stratocumulus. Part I: Thermodynamic and dynamic observations of closed cell circulations and cumulus bands. *Atmos. Res.* **54**, 117-155 (2000).

131 vanZanten, M. C. & Stevens, B. Observations of the structure of heavily precipitating marine stratocumulus. *J. Atmos. Sci.* **62**, 4327-4342, doi:10.1175/jas3611.1 (2005).

132 Comstock, K. K., Yuter, S. E., Wood, R. & Bretherton, C. S. The three-dimensional structure and kinematics of drizzling stratocumulus. *Mon. Weather Rev.* **135**, 3767-3784, doi:10.1175/2007mwr1944.1 (2007).

133 Terai, C. R. & Wood, R. Aircraft observations of cold pools under marine stratocumulus. *Atmos. Chem. Phys.* **13**, 9899-9914, doi:10.5194/acp-13-9899-2013 (2013).

134 Zuidema, P. *et al.* On Trade Wind Cumulus Cold Pools. *J. Atmos. Sci.* **69**, 258-280, doi:10.1175/jas-d-11-0143.1 (2012).

135 Savic-Jovcic, V. & Stevens, B. The structure and mesoscale organization of precipitating stratocumulus. *J. Atmos. Sci.* **65**, 1587-1605, doi:10.1175/2007jas2456.1 (2008).

136 Seifert, A. & Heus, T. Large-eddy simulation of organized precipitating trade wind cumulus clouds. *Atmos. Chem. Phys.* **13**, 5631-5645, doi:10.5194/acp-13-5631-2013 (2013).

137 Katzwinkel, J., Siebert, H. & Shaw, R. A. Observation of a Self-Limiting, Shear-Induced Turbulent Inversion Layer Above Marine Stratocumulus. *Boundary-Layer Meteorology* **145**, 131-143, doi:10.1007/s10546-011-9683-4 (2012).

138 Gerber, H. *et al.* Entrainment rates and microphysics in POST stratocumulus. *J. Geophys. Res.* **118**, 12094-12109, doi:10.1002/jgrd.50878 (2013).

139 Lu, C. S., Liu, Y. G., Yum, S. S., Niu, S. J. & Endo, S. A new approach for estimating entrainment rate in cumulus clouds. *Geophys. Res. Lett.* **39**, doi:10.1029/2011gl050546 (2012).

140 Schmeissner, T. *et al.* Turbulent Mixing in Shallow Trade Wind Cumuli: Dependence on Cloud Life Cycle. *J. Atmos. Sci.* **72**, 1447-1465, doi:10.1175/JAS-D-14-0230.1 (2015).

141 Beals, M. J. *et al.* in *Proc. 14th Conf. on Cloud Physics.* (American Meteorological Society, Boston, MA).

142 Lu, C. S., Liu, Y. G. & Niu, S. J. Entrainment-mixing parameterization in shallow cumuli and effects of secondary mixing events. *Chinese Sci. Bull.* **59**, 896-903, doi:10.1007/s11434-013-0097-1 (2014).

143 Frisch, A. S., Feingold, G., Fairall, C. W., Uttal, T. & Snider, J. B. On cloud radar and microwave radiometer measurements of stratus cloud liquid water profiles. *J. Geophys. Res.* **103**, 23195-23197, doi:10.1029/98jd01827 (1998).

144 Dong, X. Q., Ackerman, T. P. & Clothiaux, E. E. Parameterizations of the microphysical and shortwave radiative properties of boundary layer stratus from ground-based measurements. *J. Geophys. Res.* **103**, 31681-31693, doi:10.1029/1998jd200047 (1998).

145 Kollias, P., Albrecht, B. A., Lhermitte, R. & Savtchenko, A. Radar observations of updrafts, downdrafts, and turbulence in fair-weather cumuli. *J. Atmos. Sci.* **58**, 1750-1766, doi:10.1175/1520-0469(2001)058<1750:roouda>2.0.co;2 (2001).

146 Hogan, R. J., Gaussiat, N. & Illingworth, A. J. Stratocumulus liquid water content from dual-wavelength radar. *J. Atmos. Oceanic Technol.* **22**, 1207-1218, doi:10.1175/jtech1768.1 (2005).

147 Huang, D., Johnson, K., Liu, Y. & Wiscombe, W. High resolution retrieval of liquid water vertical distributions using collocated Ka-band and W-band cloud radars. *Geophys. Res. Lett.* **36**, doi:10.1029/2009gl041364 (2009).

148 Hurrell, J. W. *et al.* The Community Earth System Model A Framework for Collaborative Research. *Bull. Am. Meteorol. Soc.* **94**, 1339-1360, doi:10.1175/bams-d-12-00121.1 (2013).

149 Gettelman, A. & Morrison, H. Advanced Two-Moment Microphysics for Global Models. Part I: Off Line Tests and Comparisons with Other Schemes. *J. Climate* **28**, 1268–1287, doi:doi:10.1175/JCLI-D-14-00102.1. (2015).

150 Liu, X. *et al.* Toward a minimal representation of aerosols in climate models: description and evaluation in the Community Atmosphere Model CAM5. *Geosci. Model Dev.* **5**, 709-739, doi:10.5194/gmd-5-709-2012 (2012).

151 Bogenschutz, P. A. *et al.* Higher-Order Turbulence Closure and Its Impact on Climate Simulations in the Community Atmosphere Model. *J. Climate* **26**, 9655-9676, doi:10.1175/jcli-d-13-00075.1 (2013).

152 Grell, G. A. *et al.* Fully coupled "online" chemistry within the WRF model. *Atmos. Environ.* **39**, 6957-6975, doi:http://dx.doi.org/10.1016/j.atmosenv.2005.04.027 (2005).

153 Fast, J. D. *et al.* Evolution of ozone, particulates, and aerosol direct radiative forcing in the vicinity of Houston using a fully coupled meteorology-chemistry-aerosol model. *J. Geophys. Res.* **111**, D21305, doi:10.1029/2005JD006721 (2006).

154 Barnard, J. C., Fast, J. D., Paredes-Miranda, G., Arnott, W. P. & Laskin, A. Technical Note: Evaluation of the WRF-Chem "Aerosol Chemical to Aerosol Optical Properties" Module using data from the MILAGRO campaign. *Atmos. Chem. Phys.* **10**, 7325-7340, doi:10.5194/acp-10-7325-2010 (2010).

155 Chapman, E. G. *et al.* Coupling aerosol-cloud-radiative processes in the WRF-Chem model: Investigating the radiative impact of elevated point sources. *Atmos. Chem. Phys.* **9**, 945-964, doi:10.5194/acp-9-945-2009 (2009).

156 Yang, Q. *et al.* Assessing regional scale predictions of aerosols, marine stratocumulus, and their interactions during VOCALS-REx using WRF-Chem. *Atmos. Chem. Phys.* **11**, 11951-11975, doi:10.5194/acp-11-11951-2011 (2011).

5.0 ARM Resources Required

This section identifies facilities, instrumentation, logistical support, guest instruments, soundings, and data requested from the ARM Climate Research Facility.

Timeframe: The ACE-ENA campaign will include two 40-day aircraft IOPs for the summer (during June and July) of 2017 and the winter (during January and February) of 2018.

Location: Most of the sampling will be within 100 km of the ENA site. One potential airfield is the Lajes airport on the island of Terceira, which is about 90 km from the ENA site. We anticipate that the supplemental surface instrumentation will be deployed at the ENA facility.

Mission Length: The G-1 flight duration will be four hours or more under the anticipated meteorological conditions in the Azores.

5.1 ARM Aerial Facilities

The following is a list of requested instrumentation onboard the G-1 aircraft in addition to the standard G-1 atmospheric state and aircraft state package:

Table 1. Requested instrumentation for the G-1 aircraft.

Instrument	Measurement	Facility/Potential Contact
Aircraft Integrated Meteorological Measurement System (AIMMS-20)	5-port air motion sensing: true air speed, altitude, angle-of attack, side-slip, temperature, and RH.	AAF
Gust Probe	5-port air motion sensing: true airspeed, angle-of-attack, side-slip	AAF
Multi-Filter Radiometer	Upwelling shortwave radiation global, 415, 500, 615, 673, 870 ,940,1625 nm spectral channels	AAF
Sunshine Pyranometer, unshaded and shaded	Broadband upwelling and downwelling shortwave radiation global, broadband downwelling shortwave radiation global and diffuse	AAF
Fast-Cloud Droplet Probe (FCDP)	Cloud particles size distribution 2 to 50 µm	AAF
2-Dimensional Stereo Probe (2D-S)	Cloud particles size distribution 10 to 3,000 µm	AAF
High-Volume Precipitation Spectrometer Version 3 (HVPS-3)	Cloud particles size distribution 150 to 19,600 µm	AAF
Holographic Detector for Clouds (HOLODEC)	Cloud particle size distribution 6 to 1,000 µm	AAF
Multi-Element Water Content System (WCM-2000)	Liquid, total, and ice water content	AAF
Particle Volume Monitor-100A (PVM-100A) (Gerber probe)	Cloud liquid water content	AAF
Cloud, Aerosol, and Precipitation Spectrometer (CAPS)	Aerosol particle and cloud hydrometeor size distributions from 0.51 to 50 µm, precipitation size distributions from 25 µm to 1550 µm, and liquid water content from 0.01 to 3 g/m^3	AAF
Trace Gas Instrument System for CO and O_3	Concentrations of CO and O_3	AAF
Proton Reaction Mass – Mass Spectrometer (PTR-MS)	Volatile organic compounds (VOCs)	PNNL (John Shilling)
Fast Integrated Mobility Spectrometer (FIMS)	Aerosol size distribution, 0.01 to 0.5 µm at 1 Hz	BNL (Jian Wang)
Ultra-High-Sensitivity Aerosol Spectrometer (UHSAS)	Aerosol size distribution, 0.055 to 1 micron	AAF

Instrument	Measurement	Facility/Potential Contact
Passive Cavity Aerosol Spectrometer-100X (PCASP)	Size distribution, 0.1 to 3 μm	AAF
Condensation Particle Counter (CPC)	Total aerosol concentration >0.010 μm	AAF
Ultrafine Condensation Particle Counter (CPC)	Total aerosol concentration >0.004 μm	AAF
Dual-Column Cloud Condensation Nuclei Counter (CCN)	CCN concentrations at two specified supersaturations	AAF
3-Wavelength Particle Soot/Absorption Photometer (PSAP)	Aerosol absorption coefficient at 462, 523, 648 nm	AAF
Integrating Nephelometer, 3-Wavelengths, Model 3563	Aerosol scattering coefficient at 450, 550, 700 nm	AAF
Single-Particle Soot Photometer (SP2)	Soot spectrometry	AAF
High-Resolution Time-of-Flight Aerosol Mass Spectrometer (HR-ToF-AMS)	Non-refractory aerosol composition	PNNL (John Shilling)
Particle in Liquid Sampler	Water soluble aerosol composition	Univ. of Arizona (Armin Sorooshian)
TRAC sampling system	Particle collection on substrates	PNNL/EMSL (Alex Laskin)
Counterflow Virtual Impactor inlet (CVI)	Sampling of cloud droplet residuals	AAF
Thermal Denuder	Sampling of non-volatile component of aerosol particles	BNL (Jian Wang)

5.2 ARM Ground Facilities

Radiosondes: We request two additional radiosonde launches per day on days when the G-1 is sampling.

Guest Instrumentation Facility: We request three additional instruments to be deployed at the ENA site continuously for one year from May 1st 2017 to April 30th, 2018.

Table 2. Requested instrumentation for ground deployment.

Instrument	Measurement	Facility / Potential contact
Ultrafine Condensation Particle Counter (CPC)	Total aerosol concentration >0.003 μm	BNL (Chongai Kuang)
Scanning mobility particle size with ambient and thermal denuder inlets	Size distributions of ambient aerosol particles and non-volatile component of aerosol from 0.01 to 0.5 μm	BNL (Jian Wang/ Chongai Kuang)
Size-Resolved CCN Counter	Size-resolved CCN spectrum and particle activation efficiency	BNL (Jian Wang)

5.3 EMSL/ALS Resources

Particles collected on substrates will be brought back to the Environmental Molecular Science Laboratory (EMSL) at Pacific Northwest National Laboratory (PNNL) and Advanced Light Source (Lawrence Berkeley National Laboratory) for subsequent laboratory analyses.

ARM

CLIMATE RESEARCH FACILITY

www.arm.gov

U.S. DEPARTMENT OF ENERGY

Office of Science